JOURNAL OF GEOPHYSICAL RESEARCH, VOL. 114, A11204, doi:10.1029/2009JA014544, 2009

In situ observations of reconnection Hall magnetic fields at Mars: Evidence for ion diffusion region encounters

J. S. Halekas,[1] J. P. Eastwood,[1] D. A. Brain,[1] T. D. Phan,[1] M. Øieroset,[1] and R. P. Lin[1]

Received 8 June 2009; revised 5 August 2009; accepted 13 August 2009; published 11 November 2009.

[1] We present Mars Global Surveyor measurements of bipolar out-of-plane magnetic fields at current sheets in Mars' magnetosphere. These signatures match predictions from simulations and terrestrial observations of collisionless magnetic reconnection, and could similarly indicate differential ion and electron motion and the resulting Hall current systems near magnetic X lines. Thus, these observations may represent passages through or very near reconnection diffusion regions at Mars. Out of 28 events found at 400 km altitude with well-defined current sheet orientations, 26 have magnetic fields consistent with the expected polarities of Hall fields near diffusion regions. For these events, we find an average ratio of Hall field to main field of 0.51 ± 0.13, and an average ratio of normal to main field (reconnection rate) of 0.16 ± 0.09, consistent with terrestrial observations of reconnection. These events do not consistently correlate with the location of crustal fields or with IMF reversals, indicating that magnetic field draping alone (perhaps enhanced by high solar wind dynamic pressure) may generate current sheets capable of reconnection. For some events, we observe field-aligned electrons that may carry parallel currents that close the Hall current loop. Electron distributions around current sheets often indicate magnetic connection to the collisional exosphere. For crossings sunward of the X line, we usually observe an electron flux minimum at the current sheet, consistent with the resulting closed magnetic structure. For crossings antisunward of the X line, we do not observe flux minima, consistent with field lines open downstream. Collisionless reconnection, if common at Mars, could represent a significant atmospheric loss process.

Citation: Halekas, J. S., J. P. Eastwood, D. A. Brain, T. D. Phan, M. Øieroset, and R. P. Lin (2009), In situ observations of reconnection Hall magnetic fields at Mars: Evidence for ion diffusion region encounters, *J. Geophys. Res.*, *114*, A11204, doi:10.1029/2009JA014544.

1. Introduction

1.1. Mars Solar Wind Interaction

[2] Though Mars has no global magnetic field, it nonetheless has a magnetosphere, in which many of the same space physics processes observed in the Earth's magnetosphere operate. Unlike at Earth, where a dynamo magnetic field provides the obstacle to solar wind flow, the primary obstacle at Mars (like for Venus and comets) consists of ionized planetary atmospheric/exospheric gases [*Cloutier et al.*, 1999; *Nagy et al.*, 2004]. The solar wind is shocked and slowed upstream from this ionospheric obstacle, and the plasma flow inside the shock is generally well approximated by a gasdynamic model [*Spreiter and Stahara*, 1992; *Crider et al.*, 2004]. Magnetic field lines carried in the flow drape around the Martian ionosphere, resulting in locally near-horizontal fields on the day side, with field lines swept back into a two-lobed magnetotail extending in the flow direction on the night side [*Crider et al.*, 2004]. This magnetotail resembles the terrestrial magnetotail in morphology, but the IMF clock angle rather than a dipole field axis controls its orientation and polarity. Magnetic field draping is more ordered below the magnetic pileup boundary (MPB), with more disordered fields observed in the magnetosheath outside of the MPB [*Bertucci et al.*, 2003].

[3] The Martian magnetosphere resembles that of Venus on a global scale, though on average, the interplanetary magnetic field is weaker and much less radial (∼57° from radial as opposed to ∼35° at Venus or ∼45° at Earth), the solar wind density is lower, and the Mach number is lower. In addition, Mars' remanent crustal magnetic fields [*Acuña et al.*, 1999] perturb the interaction with the solar wind [*Mitchell et al.*, 2001; *Crider et al.*, 2002; *Brain et al.*, 2005], affecting the location of plasma boundaries. The presence of crustal fields also affects magnetic topology, with observations suggesting that the extent of topologically closed crustal field regions changes with varying IMF polarity [*Brain et al.*, 2007], presumably as a result of reconnection [*Krymskii et al.*, 2002]. Collisionless magnetic reconnection may play a key role in the Martian magnetosphere, perhaps comprising a significant atmospheric loss process.

[1]Space Sciences Laboratory, University of California, Berkeley, California, USA.

0148-0227/09/2009JA014544$09.00

[4] Recently, Mars Global Surveyor (MGS) observed in situ signatures of reconnection in a magnetotail current sheet, downstream from a crustal magnetic source [*Eastwood et al.*, 2008]. It remains unclear what role magnetic fields of solar wind, induced, and crustal origin played in this event. However, given the interplay between rapidly changing solar wind magnetic fields, draped magnetic fields in the induced magnetosphere, and crustal magnetic fields which rotate with the planet and constantly change their orientation relative to the solar wind flow, we can expect a complex and dynamic system of ever changing magnetic topology and plasma flow at Mars, with reconnection playing a potentially important role. Previously, we had only one direct observation of reconnection at Mars. Therefore, it is important to determine if this was an isolated event, or a common feature of Mars' interaction with the solar wind. In this paper, we investigate possible observations of the reconnection ion diffusion region, as identified by the characteristic Hall magnetic field signature, and describe the statistical properties of 26 such events, all located in the Martian magnetosphere, inside of the MPB.

1.2. Current Sheets in the Martian System

[5] The Martian magnetotail, much like Earth's, consists of two lobes of oppositely directed magnetic field, with a central current sheet between them. Phobos 2 first observed this structure at 2.86 R_M, and confirmed its control by the upstream IMF [*Riedler et al.*, 1991; *Yeroshenko et al.*, 1990]. Surprisingly, even at relatively low ~400 km altitudes MGS often sees the same two-lobed magnetotail structure (including the central current sheet), especially away from strong crustal magnetic fields [*Ferguson et al.*, 2005; *Halekas et al.*, 2006]. The low-altitude magnetotail current sheet has an orientation roughly consistent with the field configuration expected from draped fields in an induced magnetosphere (controlled by IMF direction), but solar wind conditions and the relative position of crustal magnetic fields also appear to affect its structure and location on the night side [*Halekas et al.*, 2006].

[6] Recently, we carried out a systematic survey of current sheets encountered by MGS outside of strong crustal field regions, using an automated procedure to identify over 10,000 current sheet crossings during the ~8 year MGS mapping mission [*Halekas and Brain*, 2009]. MGS encountered current sheets most often above the night side and in the terminator/polar regions, consistent with an origin related to magnetic field draping; however, MGS also observed a significant number of current sheets above the day side, possibly indicating solar wind discontinuities advected through the Martian system (and compressed/amplified). Dayside current sheets cluster around the perimeters of strongly magnetized crustal regions, suggesting that crustal magnetic fields may also play a role in their formation. Most current sheets observed at MGS mapping altitude have an apparent thickness of only a few hundred km, suggesting either inherently thin structures, or current sheet motion with tens of km/s velocities past the spacecraft.

[7] Observations of both ion and electron acceleration associated with current sheets in the Martian magnetosphere suggest that a variety of fundamental plasma processes operate in these regions. Both Phobos 2 and Mars Express (MEX) measured significant populations of accelerated cold planetary ions in or near the magnetotail current sheet [*Lundin et al.*, 1989; *Rosenbauer et al.*, 1989; *Fedorov et al.*, 2006, 2008]. This magnetotail ion acceleration has been variously ascribed to nonadiabatic transport [*Ip*, 1992], magnetic tension forces [*Lichtenegger et al.*, 1995; *Dubinin et al.*, 1993], and pickup processes [*Luhmann*, 1990], with the most recent observations from MEX indicating a controlling role for the convection electric field in energizing ions in the magnetotail [*Fedorov et al.*, 2006, 2008]. Meanwhile, MGS and MEX data indicate that auroral-like processes can also accelerate both ions and electrons at Mars [*Lundin et al.*, 2006; *Brain et al.*, 2006]. However, even some "auroral" events may actually be at least in part associated with magnetotail current sheets, as suggested by a recent statistical study of "auroral-like" peaked electron spectra observed by MGS [*Halekas et al.*, 2008]. Electron acceleration in some current sheets may result from magnetic field reconnection, which could drive transport and energization of photoelectrons from the dayside [*Uluşen and Linscott*, 2008]. The recent observation of in situ signatures of collisionless magnetic reconnection in a magnetotail current sheet [*Eastwood et al.*, 2008] may lend credence to this hypothesis.

[8] Given the complex and variable magnetic topology at Mars, magnetic reconnection could play an important role in controlling energy flow through the Martian system. Observations and theoretical considerations suggest a number of ways in which thin current sheets susceptible to reconnection may form in the Martian system, as shown in Figure 1. As plasma flow carries magnetic field lines through the Martian system, they drape around the ionosphere, forming current sheets between antiparallel draped field lines (Figure 1a). These induced current sheets can form anywhere in the "magnetic pole" regions and between the two lobes in the night side, depending on the degree of draping and the extent to which velocity shears cause field lines to "hang" in the ionosphere. Crustal fields may affect this scenario by slowing or deflecting tailward flow and field line transport in some regions (Figure 1d). Meanwhile, current sheets could also form directly between interplanetary field lines and crustal field lines (Figure 1b) or between stretched crustal magnetic field lines (Figure 1e). Finally, plasma flow will carry solar wind magnetic field discontinuities through the Martian system, where magnetic field lines may pile up against the ionosphere (Figure 1c) and/or crustal magnetic field regions (Figure 1f), compressing and amplifying preexisting discontinuities to form thin current sheets in the Martian magnetosphere. Each of these current sheet formation scenarios could produce a region where magnetic reconnection would subsequently take place. If significant amounts of plasma of planetary origin populate the magnetic field lines involved, these reconnection scenarios would result in losses of atmospheric gases from the Martian system.

1.3. Collisionless Magnetic Reconnection and the Ion Diffusion Region

[9] To date, most in situ observations of reconnection come from in or near the Earth's magnetosphere, or in the laboratory. However, given the ubiquity of topologically complex magnetic field configurations and dynamic plasma flows, this fundamental plasma process must operate in

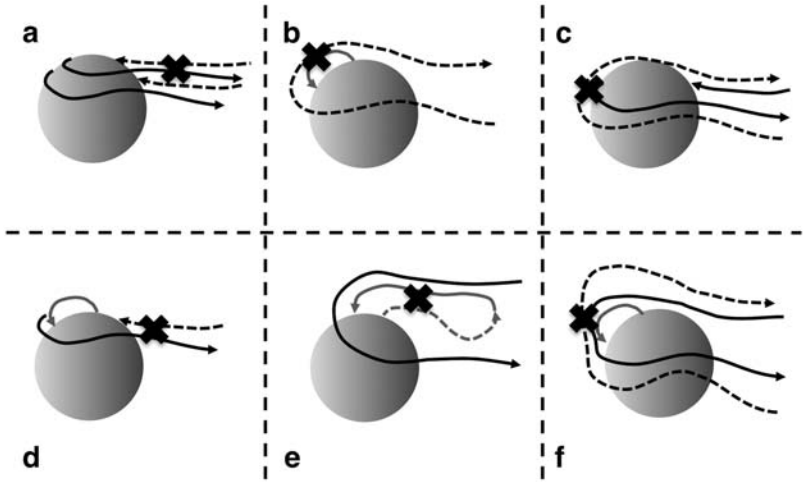

Figure 1. Possible configurations for reconnection in the Martian system, including (a) IMF draping to form an induced magnetotail current sheet, (b) direct reconnection between draped IMF and crustal fields, (c) advection and draping of a solar wind current sheet through the Martian system, (d) draping of IMF around a crustal field region to form a current sheet downstream, (e) stretching of a crustal field to form a current sheet, and eventually a detached flux rope, and (f) enhancement and thinning of a solar wind current sheet by compression over a crustal field region. For each scenario, adjacent dashed and solid lines (indicating locally opposite polarities) could reconnect, at the position marked by the thick X. IMF field lines shown in black, crustal field lines shown in gray.

many regions of the solar system and beyond. Reconnection changes magnetic topology and converts magnetic energy to particle kinetic energy, filling a key role in any dynamic space plasma environment. The importance of reconnection in Earth's magnetosphere has been long suspected [*Dungey*, 1961], and theoretical predictions of the structure of the reconnection region reached an advanced stage some time ago [*Vasyliunas*, 1975; *Sonnerup*, 1979]. However, only recently have computer simulation and observational capabilities progressed to the point where we can make detailed predictions and measurements of the kinetics of collisionless reconnection.

[10] Though many questions about the physics of reconnection remain, we have some idea of its basic mechanism and structure. Outside of the diffusion region, plasma flow carries oppositely directed magnetic fields toward one another, with both ions and electrons frozen to the field lines. Inside the diffusion region, magnetic field direction and polarity change on a small enough spatial scale that charged particles can decouple from the magnetic field, with ions decoupling first and electrons staying bound to the field longer before decoupling in a smaller region [*Vasyliunas*, 1975]. Simulations indicate that this results in a two-scale structure, with an ion diffusion region with a spatial scale on the order of the ion inertial length c/ω_{pi} surrounding a smaller electron diffusion region with a spatial scale on the order of the electron inertial length c/ω_{pe} [*Shay et al.*, 1998]. Inside this two-scale diffusion region, field lines reconnect at a magnetic X line and flow outward perpendicular to the inflow direction, accelerating plasma outflows.

[11] Inflowing ions are deflected away from the magnetic X line in the ion diffusion region, while electrons stay coupled to the field longer and penetrate further toward the neutral line, resulting in differential flow between electrons and ions that produces bipolar in-plane Hall electric fields (toward the neutral line, parallel to the inflow velocity) and Hall currents (away from the neutral line, opposite the inflow) [*Shay et al.*, 1998; *Pritchett*, 2001a, 2001b]. The nonzero divergence of these Hall currents implies that they must close via field-aligned currents outside of the diffusion region [*Treumann et al.*, 2006], and simulations suggest that the current system closes via inward electron flow (outward current) along the separatrices, and outward electron flow (inward current) in the outflow region [*Hesse et al.*, 2001; *Pritchett*, 2001b; *Shay et al.*, 2001]. The resulting current loops produce a characteristic quadrupolar out-of-plane magnetic field signature around the magnetic X line, often considered a hallmark of the importance of the Hall effect in reconnection [*Sonnerup*, 1979; *Terasawa*, 1983; *Shay et al.*, 1998; *Birn et al.*, 2001].

[12] Reconnection produces a number of observable signatures. Remote signatures of reconnection include the observation of Alfvénic jets consistent with outflow from a reconnection X line (often in coincidence with magnetic fields normal to the current sheet) at the magnetopause [*Paschmann et al.*, 1979; *Sonnerup et al.*, 1981], magnetotail [*Slavin et al.*, 1985], and in the solar wind [*Gosling et al.*, 2005], flux transfer events [*Russell and Elphic*, 1978], magnetotail flux ropes [*Elphic et al.*, 1986; *Hones et al.*, 1983] and associated traveling compression regions [*Slavin et al.*, 1984], and field-aligned electron flows [*Fujimoto et al.*, 1997; *Nagai et al.*, 2001, 2003; *Hoshino et al.*, 2001; *Owen et al.*, 2005; *Alexeev et al.*, 2005; *Manapat et al.*, 2006]. Recently, a number of authors have also reported direct encounters with the reconnection diffusion region, based on measurements of plasma flow reversals and the characteristic quadrupolar out-of-plane Hall magnetic field signatures described above [*Øieroset et al.*, 2001; *Runov et al.*, 2003; *Deng et al.*, 2004], as well as the bipolar Hall electric field signature [*Mozer et al.*, 2002; *Borg et al.*,

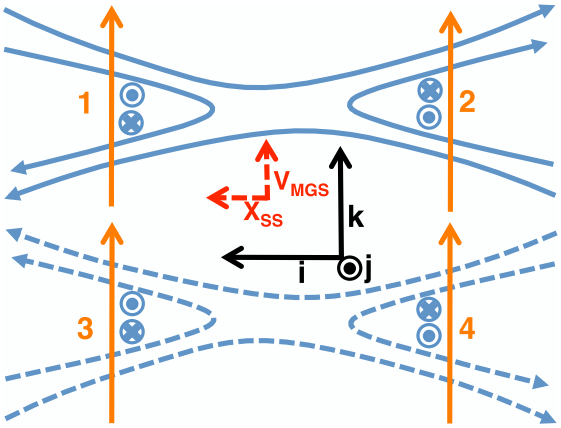

Figure 2. Schematic of four possible geometries for a spacecraft encounter with a reconnection diffusion region. We choose principal component axes (shown in black) with signs that ensure a positive dot product between the current sheet axis (maximum variance direction) and the MSO *x* axis X_{SS} (shown in red) and between the current sheet normal direction (minimum variance direction) and the spacecraft velocity vector (shown in red), with the intermediate variance axis completing a right-handed coordinate system.

2005; *Eastwood et al.*, 2007]. Many of these signatures, including Hall magnetic fields, have also been measured in the laboratory [*Ren et al.*, 2005].

[13] At Mars, no spacecraft to date has possessed the full complement of particle and fields instrumentation needed to measure all of the indicators of reconnection observed at Earth. For instance, MGS lacked ion measurements, while MEX had no magnetometer. MGS, however, did provide magnetic field and electron data sufficient to detect some of these signatures – in particular, flux ropes and Hall magnetic fields. *Eastwood et al.* [2008] described an MGS observation of a thin bifurcated sheet in the Martian magnetotail, with probable Hall magnetic field signatures, and a nearby detached flux rope structure, demonstrating that reconnection takes place in the Martian magnetosphere. In this paper, we now report on further observations of probable Hall magnetic field signatures and anisotropic electron distributions observed by MGS at current sheet crossings in the Martian magnetosphere, likely indicating encounters with reconnection ion diffusion regions. We describe several sample events, including magnetic field geometry, location, and electron characteristics. We then discuss the statistical properties of 26 such events, including their location, characteristics, and external drivers.

2. Data Sources

[14] We utilize observations from the MGS Magnetometer and Electron Reflectometer (MAG/ER) instrument [*Acuña et al.*, 2001; *Mitchell et al.*, 2001]. The MAG, consisting of two identical fluxgate magnetometers, provided vector measurements of magnetic fields, with an accuracy of ~0.5 nT in shadow, and ~1.0 nT elsewhere. The ER, a cylindrically symmetric half hemispherical "top hat" electrostatic analyzer, measured the energy and angular distributions of 10 eV to 20 keV electrons. The ER sampled electron fluxes at thirty logarithmically spaced energy channels, in sixteen 22.5° × 14° sectors, which span the entire 360° × 14° field of view. Depending on the orientation of this field of view with respect to the magnetic field direction, electron pitch angle coverage varies as a function of time and space. All magnetic field and electron data utilized in this manuscript come from the mapping phase of the MGS mission, during which the spacecraft orbited at a fixed local time of ~2am/2pm, and a nearly constant altitude of ~400 km.

3. Case Studies

3.1. Expected Magnetic Field Signatures

[15] Given a collisionless magnetic reconnection diffusion region, one can predict the Hall magnetic field configuration by considering the currents that result from the decoupling of ions and electrons, as described above in Section 1.3. In Figure 2, we show schematic views of the four possible relative positions of the current sheet and reconnection X line relative to the spacecraft trajectory, depending on the orientation of the current sheet relative to the spacecraft motion, with the expected main, normal, and out-of-plane magnetic fields. In Figure 3, we show the magnetic field components that a spacecraft would measure when passing near a reconnection diffusion region for each of these four cases. Assuming that we choose our minimum variance coordinate system with the main field roughly parallel to the MSO *x* axis (i.e., with a positive dot product), and the current sheet normal roughly aligned with the spacecraft velocity, as shown in Figure 2, we can compare spacecraft observations directly with the expected magnetic field signatures shown in Figure 3.

3.2. Case Study 1: On 21 November 2003

3.2.1. Bipolar Out-of-Plane Magnetic Fields Observed at a Martian Current Sheet

[16] In Figure 4, we show an MGS observation of a current sheet crossing above the Martian night side, located at 2am local time (i.e., toward dawn from midnight), at a solar zenith angle of 138° and a planetary longitude and latitude of 268°E, 57°N. This places the current sheet above the northern lowlands, far from any strong crustal magnetic sources. Given the subsolar location of 60°E, 21°S, most

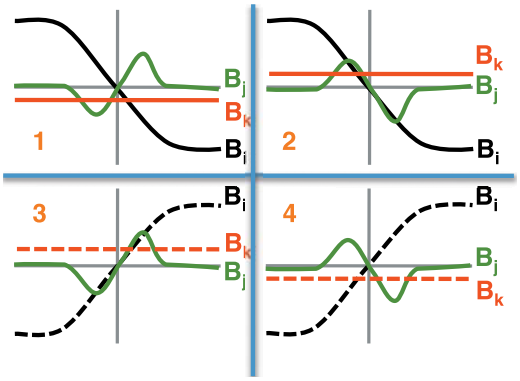

Figure 3. Expected magnetic field signature in principal components for each scenario shown in Figure 2.

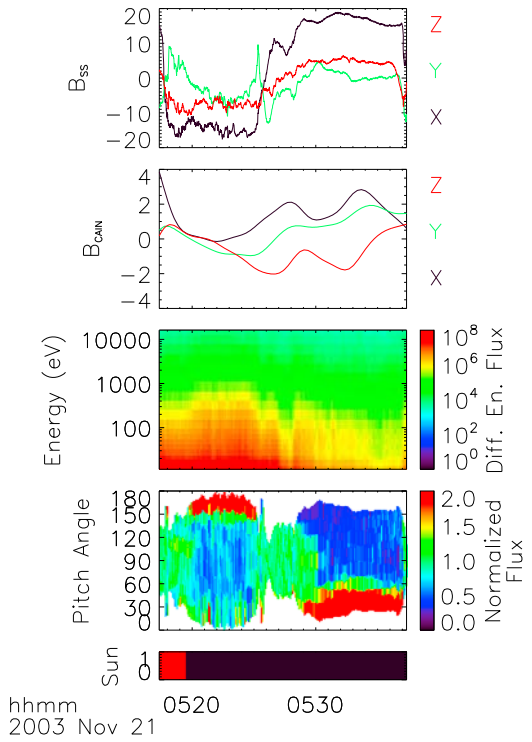

Figure 4. Nightside current sheet crossing at 05:27:20 UT on 2003/11/21, showing magnetic field components in MSO coordinates, predicted crustal field components from the Cain model, an electron differential energy flux spectrogram in ev(eV cm^2 s sr), a normalized pitch angle spectrogram for 115 eV electrons, and a color bar showing spacecraft illumination (red is the sun, black is the shadow).

strongly magnetized crustal regions sit on the dusk and/or night side of Mars at this time; thus, no strong crustal fields lie sunward from this crossing, suggesting a current sheet formation scenario that does not involve crustal magnetic fields. At the same time, we can roughly infer the IMF direction from dayside measurements in the northern hemisphere, following the methodology of *Brain et al.* [2006]. We find that the IMF draping azimuth only changes by 16° from the orbit before the current sheet crossing to the orbit after the crossing, suggesting a roughly constant IMF clock angle, and reducing the chance that this current sheet formed as a result of a large-scale discontinuity of solar wind origin. Thus, this current sheet most likely formed via antiparallel magnetic field draping in the induced magnetotail, as shown in Figure 1a.

[17] The magnetic field observed during this crossing lies primarily in the MSO x direction (MSO coordinates are defined with x toward the Sun, z perpendicular to the ecliptic, and y completing the right-handed coordinate system, nearly antiparallel to Mars' orbital velocity), consistent with the typical magnetic field draping pattern in Mars' induced magnetotail [*Halekas and Brain*, 2009]. The small local crustal magnetic field components (~2–3 nT, compared to a main field of ~20 nT) estimated from the Cain model [*Cain et al.*, 2003] confirm that crustal field influences likely will not prove significant at this location, though we cannot completely rule out a role for these small fields. As MGS crosses the current sheet, indicated by the reversal of the main field component, we observe a bipolar out-of-plane magnetic field signature aligned primarily in the MSO y direction. This bipolar signature has a peak magnitude of ~10 nT, about half that of the main field. Unfortunately, MGS does not have ion measurements that could be used to detect Alfvénic outflow jets to provide further evidence for the presence of a reconnection X line. However, the bipolar out-of-plane magnetic field signature appears qualitatively and quantitatively very similar to those observed in reconnection diffusion regions at the Earth's magnetotail [*Øieroset et al.*, 2001; *Runov et al.*, 2003; *Borg et al.*, 2005], and magnetopause [*Mozer et al.*, 2002; *Vaivads et al.*, 2004], and magnetosheath [*Phan et al.*, 2007].

[18] This bipolar out-of-plane magnetic signature can be interpreted as a spacecraft crossing of two branches of the quadrupolar Hall current loop structure in the ion diffusion region, located near the magnetic X line, as shown in Figure 2. If the observed magnetic fields do indeed represent the signature of the Hall current loop structure, they indicate that the spacecraft passed rather near the magnetic X line (in or very near the ion diffusion region), since we observe essentially no separation between positive and negative out-of-plane magnetic signatures [*Phan et al.*, 2007].

[19] In Figure 5, we show an expanded view of the time period around the current sheet crossing shown in Figure 4, with the magnetic field now rotated into a minimum variance coordinate system [*Sonnerup and Cahill*, 1967]. We also display hodograms of the magnetic field in this same coordinate system in Figure 6. In minimum variance coordinates, we clearly see the very symmetric bipolar out-of-plane magnetic signature, in addition to the presence of a superposed guide field of a few nT. The normal field component, meanwhile, though variable in magnitude, remains consistent in direction throughout the current sheet crossing. The large (>7) ratios of the eigenvalues from minimum variance analysis, and the consistency of the magnetic field components throughout the current sheet crossing, imply a well-defined current sheet orientation and structure.

3.2.2. Event Geometry

[20] If we can reliably measure all of the magnetic field components across a current sheet structure, we can determine the basic current sheet properties and the location of the observation relative to the magnetic X line. If we assume that the current sheet remains stationary for the entire duration of the crossing, we can use the observed duration of the current sheet crossing, along with the orientation derived from the minimum variance analysis, to determine its thickness. Since the current sheet likely does move at least slightly, this procedure provides only a minimum thickness estimate. Boundary motions may be as large as 10's of km/s, in analogy with terrestrial observations, in which case our minimum thickness estimate could prove far smaller than the true thickness of the current sheet. However, the scale of boundary motions this close to the planet in an induced magnetosphere is unknown and difficult to estimate. For this current sheet, we estimate the crossing duration by measuring the temporal extent of the reversal in the main field component (~70 s), multiplying by the spacecraft velocity (~3.4 km/s), and multiplying by the

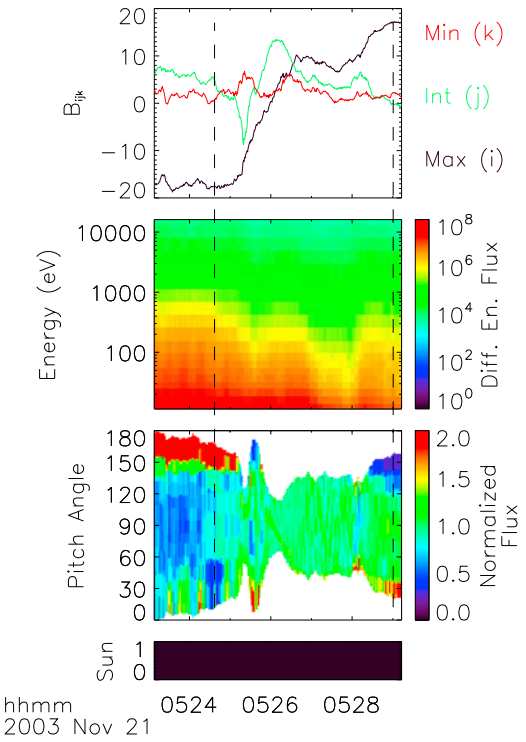

Figure 5. Expanded view of the current sheet crossing in Figure 4, showing magnetic field in minimum variance coordinates, electron differential energy flux in ev(eV cm^2 s sr), normalized pitch angle distribution at 115 eV, and color bar showing spacecraft illumination (red is the sun, black is the shadow). Minimum variance analysis for this time period indicates principal component axes i,j,k = [0.95, 0, 0.31], [0.04, −0.99, −0.14], [0.31, 0.15, −0.94] in MSO coordinates, with eigenvalues λ_i = 170, λ_j = 14.4, λ_k = 1.96. Magnetic field components suggest a crossing of type 3, sunward from the X line. Dashed lines indicate times of pitch angle distributions shown in Figures 7 and 8.

dot product of the normal and the spacecraft velocity vector (0.36), to derive a minimum current sheet thickness T = ∼85 km.

[21] Measurements of plasma density and temperature in the magnetotail have proven difficult, but given typical magnetosheath plasma densities of 1 cm^{-3}, electron temperatures of ∼10 eV, and proton temperatures of ∼50 eV estimated by MEX [*Franz et al.*, 2006], we can obtain a rough estimate of plasma length scales. Given a magnetic field strength of ∼20 nT, we expect typical thermal proton and electron gyroradii of ∼50 km and 0.5 km respectively in the sheath, possibly implying even smaller gyroradii in the magnetotail, where slightly lower temperatures may prevail. We thus estimate a minimum current sheet thickness of the same order as the expected proton gyroradius, but smaller than heavy ion gyroradii. Meanwhile, we expect proton and electron inertial lengths of ∼230 km and ∼5 km respectively in the sheath, implying larger characteristic scale sizes in the magnetotail, where we expect to find even lower plasma densities. Therefore, we estimate that the current sheet has a minimum thickness comparable to (or even smaller than) the ion inertial length, a condition typically thought to favor reconnection.

[22] We can obtain a rough estimate of the linear distance d along the current sheet from the crossing point to the reconnection X line, assuming that magnetic field components remain roughly constant near the X line on both sides of the neutral line, and that the current sheet has zero thickness at the X line (it likely has finite thickness, so this estimate gives an upper bound). Given the current sheet thickness T, and the normal and main field components B_k and B_i, we can estimate that $d = T/2*\langle B_k\rangle/\langle B_i\rangle$ = ∼400 km, assuming that magnetic field lines extend in a straight line from the observation point to the X line. Assuming a typical ion diffusion region width of several ion inertial lengths [*Mozer et al.*, 2002], this estimate implies that the spacecraft very likely passes directly through the ion diffusion region, consistent with the observation of back-to-back bipolar out-of-plane fields (i.e., no separation between the two polarities).

[23] Finally, by looking at the sign of the magnetic field components and comparing to the expected signatures shown in Figure 3, we can determine where the crossing took place relative to the magnetic X line. For the current sheet crossing shown in Figures 4 and 5, we find that the magnetic field signature indicates a crossing of type 3, sunward from the magnetic X line.

[24] All of the analyses described in the preceding paragraphs assume that the current sheet remains nearly stationary as the spacecraft crosses it. On the other hand, if the current sheet actually overtakes the spacecraft, then it invalidates our determination of the position relative to

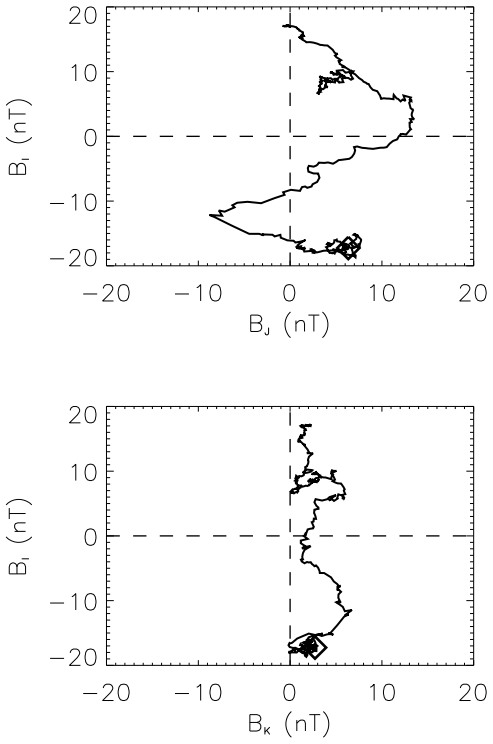

Figure 6. Hodograms of magnetic field components in minimum variance coordinates, for the same time period shown in Figure 5. (top) Maximum and minimum variance components and (bottom) maximum and intermediate variance components.

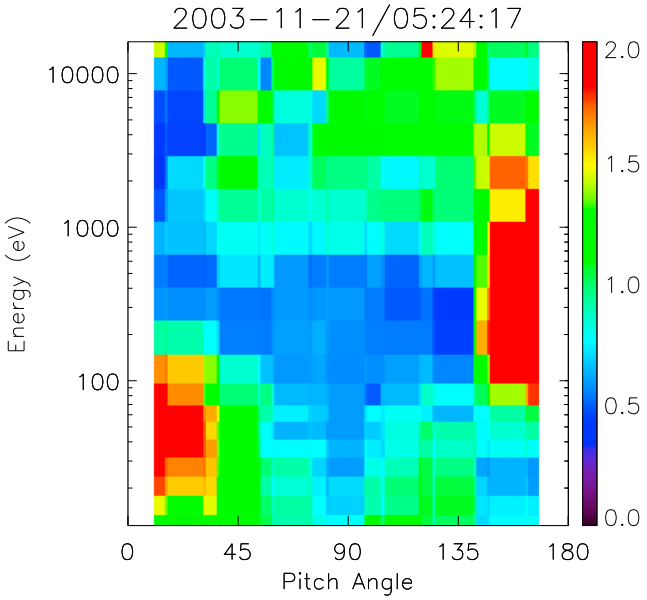

Figure 7. Normalized pitch angle distributions as a function of energy, before the current sheet crossing shown in Figures 4 and 5. Low energy field-aligned electrons flow antisunward (toward the X line implied by magnetic field components) and high energy electrons flow sunward (away from the X line).

the X line. In this case, we would observe the two polarities of main and out-of-plane components of the field in the opposite sequence from what we expect (since the spacecraft velocity relative to the current sheet would be opposite to expectations), but would still observe the same sign for the normal field component. We would therefore, for instance, erroneously identify a current sheet crossing of type 2 (antisunward from the X line) as a crossing of type 3 (sunward from the X line). We cannot rule out such a false characterization of the current sheet orientation; however, if the current sheet does overtake the spacecraft, this places some restrictions on the global morphology of the Martian magnetotail. In particular, if we assume a quasi-steady current sheet structure, then if it overtakes the spacecraft during one part of the orbit, we expect the spacecraft to recross the current sheet at some other point during the same orbit, unless the current sheet normal is nearly aligned with the orbit normal (not the case for this event). This does not occur during the time period in question. Therefore, we cannot conclude that the current sheet overtakes the spacecraft unless we assume a transient current sheet structure that sweeps past the spacecraft only once. We cannot rule out this scenario based on one observation, but the small change in IMF draping azimuth argues against it. In addition, we shall show later in this paper (in Section 4.5) that the consistency in the observed electron fluxes during for similar events also argues against this possibility.

3.2.3. Electron Signatures

[25] Though the magnetic field observations already provide convincing evidence for reconnection, electron energy spectra and pitch angle distributions may provide an additional diagnostic of the presence of reconnection at Mars. Unfortunately, the 2d measurements provided by the MGS ER do not, in general, cover the full range of pitch angles. Therefore, we can generally only make tentative conclusions about the angular distributions of electrons. Electron energy spectra provide more unambiguous information, though the possible presence of high-flux beams in regions of phase space not covered by our measurements still ensures some ambiguity. Nonetheless, electron observations can provide important information about the physics of the events studied here. We therefore investigate the electron fluxes observed in and around the current sheet crossing shown in Figures 4 and 5. MGS observes larger electron fluxes on one side of the current sheet than on the other, suggesting the possibility of asymmetric reconnection (despite the highly symmetric magnetic signatures). In addition to this overall trend, we find a clear bifurcated minimum (with deepest minima at 5:25:30 and 5:28:00) in electron flux near the current sheet crossing itself. Given the narrowness of the current sheet crossing and the asymmetric structure of the electron flux, it is difficult to conclusively associate the electron density minimum with either the current sheet itself or with the nearby magnetic separatrices. Simulations [*Shay et al.*, 2001; *Pritchett*, 2001b; *Yang et al.*, 2006] and some observations [*Mozer et al.*, 2002; *Øieroset et al.*, 2001] indicate the presence of a plasma density depletion along the magnetic separatrices, possibly resulting from a strong Hall effect or equivalently a current sheet thickness scale small compared to the ion inertial length [*Yang et al.*, 2006]. Thus, the presence of reduced electron fluxes along the separatrices may prove wholly consistent with the inferred thin current sheet structure. However, though some observations do suggest depletions in both electrons and ions [*Vaivads et al.*, 2004], models suggest that the depletion along the separatrices should primarily be observed in the ions [*Shay et al.*, 2001; *Yang et al.*, 2006]. Alternatively, reduced electron fluxes may simply indicate that the current sheet field lines connect to the planet or thread through the collisional exosphere at some point sunward from the crossing. This configuration, along with the inferred crossing location sunward from the magnetic X line, would imply flux tubes closed at the antisunward end and connected to a plasma absorption region at the sunward end, allowing the evacuation of plasma from these regions.

[26] At this time, MGS's orientation relative to the magnetic field direction fortuitously allowed fairly complete pitch angle measurements over much of the interval in question. For 115 eV electrons, we observe nearly isotropic pitch angle distributions in the current sheet (at least over the pitch angle range covered by the instrument at this time), but highly anisotropic field-aligned electrons on both sides of the current sheet. These field-aligned electrons travel sunward (toward Mars) along magnetic field lines on both sides of the current sheet. This type of electron signature has been noted before at Mars, and suggested as a potential remote indicator of the presence of reconnection, [*Halekas and Brain*, 2009].

[27] During the time period shown in Figures 4 and 5, electron angular distributions vary dramatically as a function of energy. We show sample electron pitch angle distributions (self normalized for each energy in order to best display electron anisotropy) as a function of energy from times before and after the current sheet crossing in Figures 7 and 8. We find that, before the current sheet

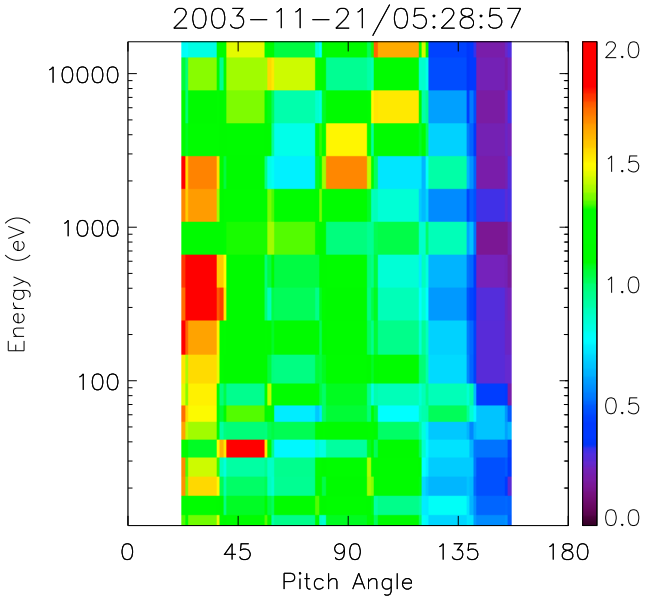

Figure 8. Normalized pitch angle distributions as a function of energy, after the current sheet crossing shown in Figures 4 and 5. Electrons of all energies flow sunward (away from the X line) and a loss cone distribution suggests magnetic field lines that pass through a collisional region of the Martian exosphere.

crossing, electrons from ~100–1000 eV flow sunward (away from the inferred X line location, and toward Mars), while electrons below ~100 eV flow antisunward (toward the inferred X line location). After the current sheet crossing, electrons of all energies flow sunward (away from the inferred X line location, and toward Mars), and a loss cone centered around 180° pitch angle indicates probable magnetic connection to the collisional exosphere.

[28] These electron pitch angle signatures show significant similarities to those observed in the terrestrial magnetotail [see, e.g., *Manapat et al.*, 2006], where coincident low-energy electron flows toward the magnetic X line and energetic electron flows away from the X line are commonly interpreted as signatures of a field-aligned current system that closes the Hall current loop. Thus, it is tempting to conclude that the field-aligned electron fluxes observed at Mars similarly represent manifestations of an extended Hall current structure. However, several factors lead us to question this identification. First and foremost, simulations show that the low energy electrons that close the Hall current loop should primarily flow into the reconnection region along the magnetic separatrices [see, e.g., *Shay et al.*, 2001]. Thus, one would expect that the field-aligned electron signatures that we observe at Mars should similarly remain localized to the region of the separatrices, rather than extending to a significant distance from the neutral sheet as we observe (see Figure 4).

[29] In addition, we very commonly observe similar electron signatures, with field-aligned electron distributions at 115 eV found near (on at least one side of) ~13% of the current sheet crossings identified by MGS, and often extending to large distances from the current sheet. Of these field-aligned electron observations, 25% display the same reversal in polarity relative to the magnetic field at the neutral sheet. The prevalence of this type of electron distribution greatly exceeds the frequency of bipolar magnetic field signatures, which we observe at only ~0.25% of current sheet crossings. This lack of a correlation does not present an insurmountable objection, since at most times we may pass through the current sheet far from the diffusion region (thus not observing the Hall magnetic signature), but it does cast further doubt on the association of field-aligned electrons in the Martian magnetotail with reconnection events.

[30] On the other hand, we find it difficult to explain these field-aligned electrons, especially those with a polarity reversal at the current sheet, in any other fashion. Absent the polarity reversal, field-aligned electrons in the Martian magnetosphere could represent anisotropic solar wind strahl electrons that enter the magnetosphere along interplanetary magnetic field lines [*Dubinin et al.*, 1994]. However, in order to explain the polarity reversal at the current sheet, one must suppose the presence of bidirectional strahl, with one polarity of the strahl entering along the magnetosphere along the field lines on each side of the current sheet. Bidirectional strahl is typically associated with unique closed magnetic field geometries such as magnetic clouds and CME's [*Gosling*, 1990; *Gosling et al.*, 1993]. We cannot rule out these scenarios, but they seem less likely to explain all of our observations. Thus, we have no clearly correct explanation for the observed field-aligned electrons. We know little enough about the details of the Martian magnetotail that some other mechanism entirely, such as parallel electric fields, could very conceivably explain these electron features. In any case, we feel that we cannot draw any firm conclusions from the field-aligned electrons we observe, though in some cases they do appear consistent with the expected electron flows in and around a reconnection diffusion region. Therefore, the bipolar out-of-plane magnetic signatures remain our strongest evidence for reconnection.

3.3. Case Study 2: On 30 March 2001

3.3.1. Magnetic Field Signatures

[31] For comparison, Figure 9 shows a second current sheet crossing with similar out-of-plane magnetic field signatures, but somewhat different electron characteristics. This crossing also occurred on the night side, at a local time of 2am, and a solar zenith angle of 140°. Given the geographic longitude and latitude of 358°E, 42°S, and the subsolar location of 143°E, 17°N, this crossing should also lie some distance from any significant crustal fields, with any significant crustal field regions located downstream. Similarly to the first case, we find that the IMF draping azimuth only changes by 22° from the orbit before the current sheet crossing to the orbit after the crossing, suggesting a roughly constant IMF clock angle. Thus, this current sheet also likely formed via antiparallel magnetic field draping in the induced magnetotail, as in Figure 1a. Similarly to the first example, the main field lies mainly along the MSO x axis. However, the out-of-plane bipolar magnetic field signature lies between the MSO y axis and z axis, rather than mainly along the y axis as in the previous example. As before, using the Cain model, we predict only weak crustal fields near the current sheet crossing itself. We do see moderate crustal fields not too far from the crossing,

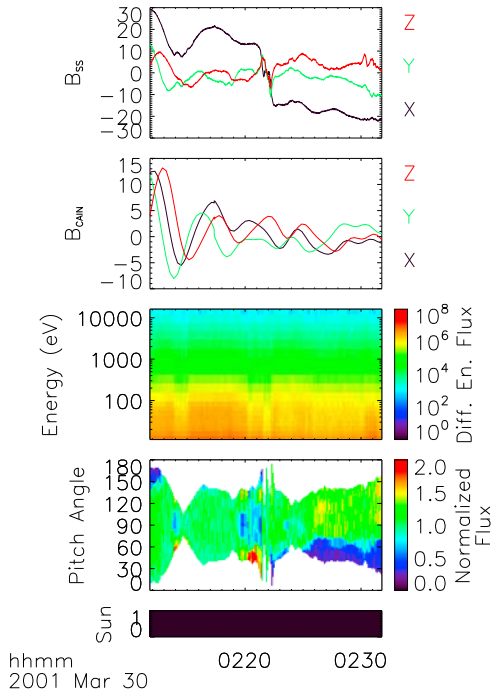

Figure 9. Nightside current sheet crossing at 02:21:47 UT on 2001/03/30, showing magnetic field components in MSO coordinates, predicted crustal field components from the Cain model, an electron differential energy flux spectrogram in ev(eV cm^2 s sr), a normalized pitch angle spectrogram for 115 eV electrons, and a color bar showing spacecraft illumination (red is the sun, black is the shadow).

but since they lie antisunward, they likely should not significantly affect the magnetic field draping and current sheet dynamics.

[32] We show an expanded view of the time period around the crossing, in Figure 10, with the magnetic fields now displayed in a minimum variance coordinate system. We also display a hodogram of the magnetic field in these coordinates in Figure 11. As in the first case, the ratio of the minimum variance eigenvalues and the consistency of the magnetic field components indicate a well-defined current sheet orientation and structure. We can perform similar analyses of the current sheet orientation and structure, thereby estimating a minimum current sheet thickness T = ~185 km, and a linear distance along the current sheet to the X line d = ~900 km, both about double the values in the first case (as always, assuming a stationary current sheet). Finally, according to the polarity of the magnetic signatures (assuming the current sheet does not overtake the spacecraft), this crossing lies sunward from the X line, just as in the first case.

[33] Though this current sheet closely resembles the case considered above, we find some differences in morphology. Both the main field and the out-of-plane component show a reduction in slope near the center of the crossing, with a clear plateau in the main field. Since the main field has a much more significant plateau than the out-of-plane component, this cannot be purely a result of current sheet motion, and thus the observations strongly suggest a bifurcated current sheet (thought to favor reconnection).

3.3.2. Electron Signatures

[34] The overall morphology of the electron fluxes proves very similar to the first event, with a bifurcated minimum in electron flux observed, centered on the neutral sheet. Pitch angle distributions of electrons at 115 eV show field-aligned flows sunward (toward Mars) before the crossing, nearly isotropic electrons in and around the current sheet itself, and a loss cone distribution indicating likely magnetic connection to the collisional exosphere after the crossing. However, when we investigate the pitch angle signatures as a function of energy in Figures 12 and 13, we find some surprising differences from the first event. Before the crossing, we find low energy electrons that flow sunward (away from the inferred X line), and counterstreaming electrons at higher energies. After the crossing, we also find low energy electrons flowing sunward (away from the inferred X line), and higher energy electrons flowing antisunward (toward the inferred X line). This electron angular signature appears opposite in most respects to that in the first event, and opposite to the characteristics of electrons expected in the Hall current loop and observed at Earth in similar geometries. These field-aligned electron distributions could only

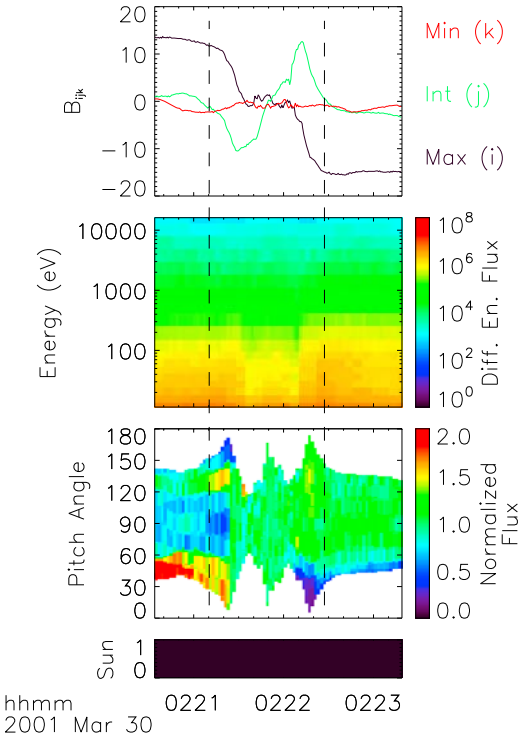

Figure 10. Expanded view of the current sheet crossing in Figure 9, showing magnetic field in minimum variance coordinates, electron differential energy flux in ev(eV cm^2 s sr), normalized pitch angle distribution at 115 eV, and color bar showing spacecraft illumination (red is the sun, black is the shadow). Minimum variance analysis for this time period indicates principal component axes i,j,k = [0.99, 0.14, −0.06], [0.07, −0.76, −0.65], [−0.14, 0.64, −0.76] in MSO coordinates, with eigenvalues λ_i = 129, λ_j = 22.4, λ_k = 0.50. Magnetic field components suggest a crossing of type 1, sunward from the X line. Dashed lines indicate times of pitch angle distributions shown in Figures 12 and 13.

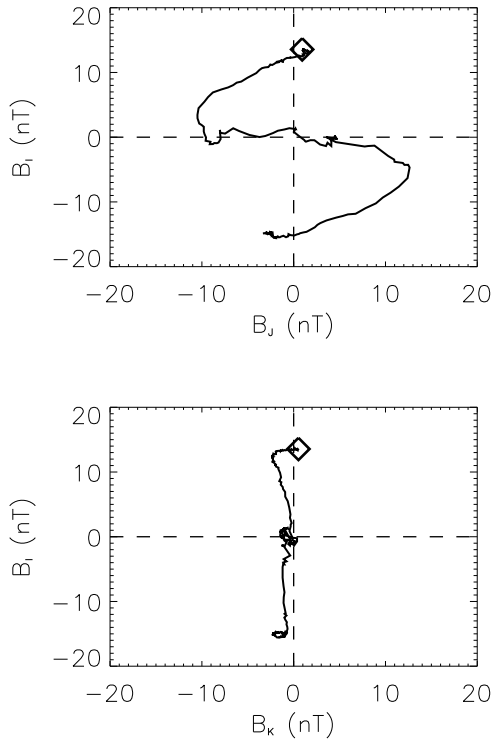

Figure 11. Hodograms of magnetic field components in minimum variance coordinates, for the same time period shown in Figure 10. (top) Maximum and minimum variance components and (bottom) maximum and intermediate variance components.

conform to expectations from terrestrial observations if the magnetic X line actually lay sunward from the crossing, rather than antisunward as we inferred from the magnetic field components.

[35] Thus, we have evidence from the magnetic field signature that this second crossing lies sunward from the X line, but some indications from field-aligned electron flows that the crossing could actually be antisunward. We could resolve this contradictory evidence if the current sheet overtakes the spacecraft, causing us to falsely identify the location of the crossing relative to the X line. However, for the reasons discussed above in Section 3.2.2, we do not favor this interpretation. Furthermore, if this crossing did lie antisunward from the X line, and our estimates of the linear distance along the current sheet to the X line of ~900 km prove correct, the combination of the high solar zenith angle of the crossing and the main field alignment nearly along the Mars-Sun line would place the X line well below Mars' surface, a physical impossibility. We therefore conclude that the field-aligned electron signatures at Mars may not correspond in a simple way to those observed in the Hall current loop in the terrestrial magnetosphere. As discussed above, the nonlocalization of the field-aligned electron flows at Mars, and the lack of any clear association with other signatures of reconnection, may imply that they do not actually correspond to carriers of the parallel currents that close the Hall current loops at Mars. Thus, the out-of-plane magnetic field signatures remain the best diagnostic of reconnection for our events.

4. Event Statistics

4.1. Event Selection

[36] The two events described in the preceding section represent only two out of a larger sample of similar events. We surveyed over 10,000 current sheet crossings identified in a previous study [*Halekas and Brain*, 2009], and visually identified 56 instances of significant bipolar out-of-plane magnetic field signatures at current sheet crossings. Of these

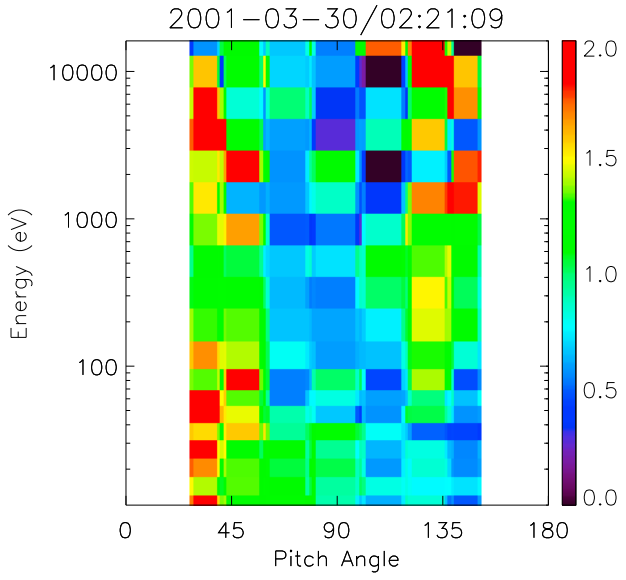

Figure 12. Normalized pitch angle distributions as a function of energy, before the current sheet crossing shown in Figures 9 and 10. Low energy field-aligned electrons flow sunward (away from the X line implied by magnetic field components) and high energy electrons counterstream.

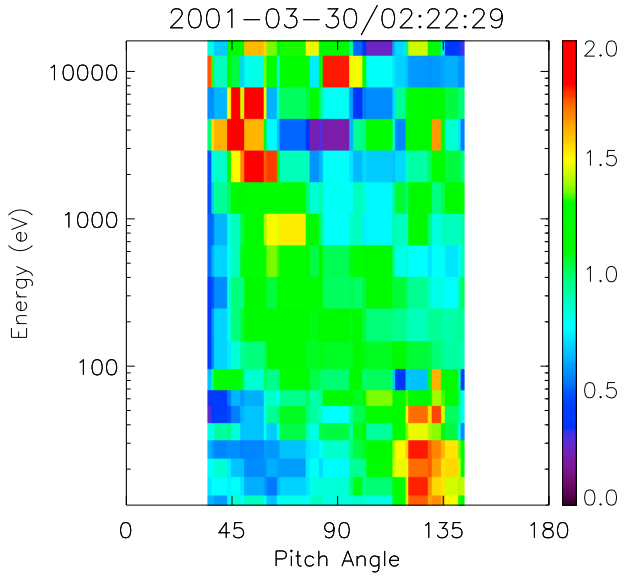

Figure 13. Normalized pitch angle distributions as a function of energy, after the current sheet crossing shown in Figures 9 and 10. Low energy electrons flow sunward (away from the X line) and high energy electrons flow antisunward (toward the X line).

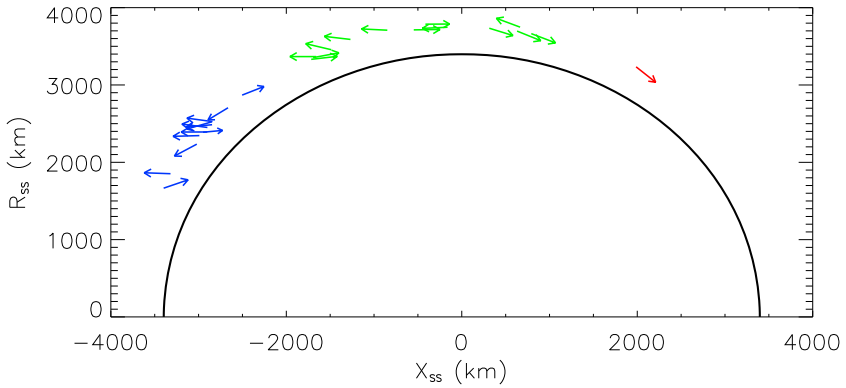

Figure 14. All 26 events, plotted in cylindrical MSO coordinates (with $R^2 = Y^2 + Z^2$). Red indicates dayside crossings, green indicates terminator/polar region crossings, and blue indicates nightside crossings. Arrows point along the current sheet axes toward the X lines implied by magnetic field components.

56 instances, 18 cases had very noisy magnetic fields, a fluctuating normal field, or a very asymmetric magnetic field signature, and we therefore eliminated them from our study. For the remaining 38 events, we conducted minimum variance analyses, and eliminated any events with poorly determined normal fields or normal orientations. Specifically, we eliminated events with average normal magnetic fields less than 0.5 nT, or with normal fields less than 1 nT and having a fractional uncertainty greater than 30% (thus ensuring that we can determine the polarity of the normal field correctly even in the presence of the worst case magnetic field errors), or with ratios of minimum to intermediate eigenvectors of greater than 30%. It is important to note that these criteria result in the selection of only relatively intense reconnection events, with large values of $B_{normal}/|B|$. The true number of reconnection events may prove much larger than the small data set that we have selected. In any case, this down selection resulted in the elimination of 10 additional events, leaving 28 events. Of these 28 events, only two events had fields with polarities inconsistent with the expected signature of a Hall current structure, and we likewise eliminated these events. Therefore, we finally selected 26 current sheet crossings (12 on the night side, 13 in the terminator/polar regions, and one on the day side) with clean magnetic field measurements, well-defined current sheet orientations and normal fields, and field signatures consistent with the expected signature of a Hall current structure (as shown schematically in Figures 2 and 3). We display the location of these current sheet crossings in cylindrical MSO coordinates and geographic coordinates in Figures 14 and 15, and list their basic properties in Table 1.

4.2. Basic Event Properties

[37] The fact that, out of 28 bipolar field events with clean magnetic field signatures, 26 have field polarities consistent with Hall fields in and around a reconnection diffusion region, provides strong evidence that these events do indeed represent encounters with reconnecting current sheets. In addition, for all but three of the events, the positive and negative lobes of the bipolar signature are back to back, with essentially no gap between them, indicating that the spacecraft likely passed very near a reconnection diffusion region.

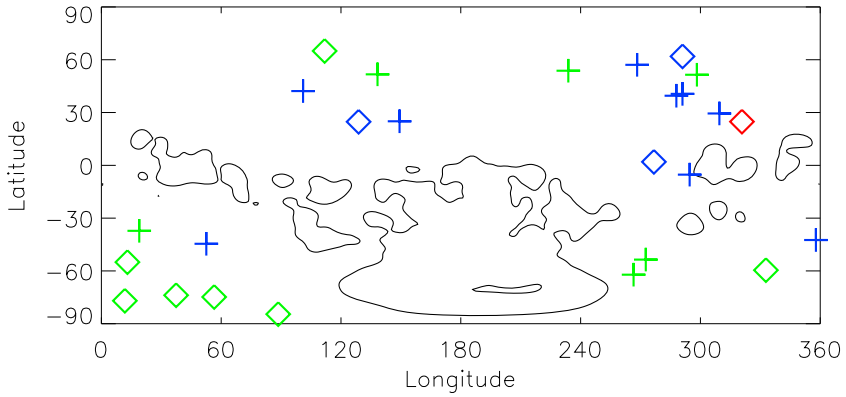

Figure 15. All 26 events, plotted as a function of geographic location. Contour lines indicate the 20 nT crustal field magnitude level from the Cain model. Red indicates dayside crossings, green indicates terminator/polar region crossings, and blue indicates nightside crossings. Diamonds show crossings antisunward of the X line, pluses show crossings sunward of the X line as implied from magnetic components.

Table 1. Event List

Date and Time[a]	SZA	Longitude and Latitude	Subsolar Longitude and Latitude	Position Relative to X Line by B (Electron)	115 eV Electron Before/After	115 eV Electron During	Peak $\lvert B_i\rvert/\langle\lvert B_i\rvert\rangle$	$\langle\lvert B_k\rvert\rangle/\langle\lvert B_i\rvert\rangle$
2005-06-26/03:50:38	58	321, 25	284, −21	Antisunward (Sunward)	Mixed/Noisy	Isotropic/Noisy	0.60	0.072
2001-11-23/09:47:40	78	12, −77	179, −25	Antisunward (Sunward)	Antisunward FA/ Isotropic	Isotropic	0.47	0.175
2001-11-04/20:19:51	80	37, −74	199, −25	Antisunward	Anti-Sun FA/Isotropic	Isotropic	0.69	0.060
2003-11-30/00:08:37	85	56, −75	225, −20	Antisunward	Loss Cone/Isotropic	Isotropic	0.60	0.107
2005-02-04/11:20:42	96	112, 65	243, 10	Antisunward (Sunward)	Isotropic	Isotropic	0.65	0.201
2005-05-31/22:37:08	98	333, −60	116, −16	Antisunward	Isotropic	Isotropic	0.53	0.087
2001-06-21/06:39:55	117	13, −55	157, −1	Antisunward (Antisunward)	Isotropic/ Loss Cone	Isotropic	0.34	0.136
2003-01-06/01:41:19	117	89, −85	266, 22	Antisunward	Isotropic	Isotropic	0.52	0.106
2005-07-09/00:05:57	80	138, 52	106, −23	Sunward (Sunward)	Noisy Isotropic/ Sunward FA	Isotropic	0.46	0.086
2004-11-12/06:56:55	92	267, −62	221, 23	Sunward (Sunward)	Bidirectional/Isotropic	Trapped	0.49	0.335
2001-03-29/06:13:25	103	298, 51	77, 17	Sunward (Sunward)	Loss Cone	Isotropic, Flux Decrease	0.32	0.094
2001-05-20/20:18:43	109	234, 54	10, 6	Sunward (Sunward)	Bidirectional/ Loss Cone	Isotropic, Flux Decrease	0.64	0.132
2001-11-12/02:46:47	113	19, −37	174, −25	Sunward	Loss Cone/ Isotropic	Isotropic/ Flux Increase	0.38	0.136
2003-05-12/00:25:53	116	273, −54	54, −1	Sunward	Sunward FA	Trapped/ Flux Decrease	0.38	0.30
2001-09-25/02:19:23	131	291, 62	70, −22	Antisunward (Antisunward)	Isotropic/Loss Cone	Isotropic	0.29	0.31
2003-07-24/09:32:01	141	129, 25	267, −18	Antisunward (Antisunward)	Noisy Loss Cone/ Isotropic	Mixed/ Flux Increase	0.38	0.196
2004-03-19/09:09:14	154	277, 2	71, 3	Antisunward (Antisunward)	Loss Cone	Isotropic/ Flux Increase	0.43	0.074
2006-03-17/04:58:19	135	149, 25	301, 11	Sunward	Mixed/Loss Cone	Mixed/ Flux Decrease	0.63	0.081
2003-11-21/05:27:20	138	268, 57	60, −21	Sunward (Sunward)	Sunward FA	Isotropic/ Flux Decrease	0.63	0.326
2006-01-02/20:42:48	138	288, 40	84, −4	Sunward	Sunward FA	Isotropic	0.36	0.097
2001-11-03/02:45:07	139	295, −5	86, −25	Sunward (Antisunward)	Isotropic/ Loss Cone	Trapped/ Flux Decrease	0.59	0.264
2001-03-30/02:21:47	140	358, −42	143, 17	Sunward (Antisunward)	Sunward FA/ Loss Cone	Isotropic, Flux Decrease	0.76	0.090
2003-07-20/19:11:49	140	310, 29	87, −18	Sunward	Sunward FA	Isotropic	0.50	0.084
2005-07-08/14:45:45	142	101, 42	241, −23	Sunward	Sunward FA	Isotropic/ Flux Decrease	0.58	0.229
2004-11-03/02:45:13	143	53, −45	196, 24	Sunward (Antisunward)	Isotropic	Mixed	0.61	0.227
2005-10-11/15:04:44	151	289, 41	86, −21	Sunward	Loss Cone/ Sunward FA	Isotropic	0.38	0.140

[a]Date and time format is year-month-day/time and time is in UT.

[38] For each event, we calculate the ratio of the Hall field to the main field (we calculate the average value, with any guide field removed, by dividing the peak-to-peak distance between the out-of-plane field peaks on each side of the current sheet by the total main field jump from one side of the current sheet to the other), finding an average ratio of 0.51, with a standard deviation of 0.13. These Hall field amplitudes are comparable in size to observations at Earth [e.g., *Øieroset et al.*, 2001; *Mozer et al.*, 2002; *Phan et al.*, 2007]. We also calculate the ratio of normal field to main field magnitude, which can be interpreted as the reconnection rate. We find an average ratio of 0.16, with a standard deviation of 0.09. This reconnection rate indicates that reconnection at Mars is in the regime of fast reconnection, similar to that at Earth. This rate is somewhat larger than that typically observed at the terrestrial magnetosphere and magnetotail, possibly because of our selection criteria, which strongly favors intense reconnection events. We list the individual ratios for each event in Table 1.

4.3. Event Distribution

[39] For each event, we use magnetic field components to determine the location of the crossing relative to the magnetic X line, as described above. For cases where we observe oppositely directed field-aligned flows of high and low energy electrons before and/or after the crossing, we also utilize these to infer the location of the X line, subject to the assumption that low energy electrons flow toward the X line, and high energy electrons flow away from the X line, as in the terrestrial magnetosphere. As shown in Table 1, we see these electron signatures for a little over half of the events. Often the X line location inferred from the electrons

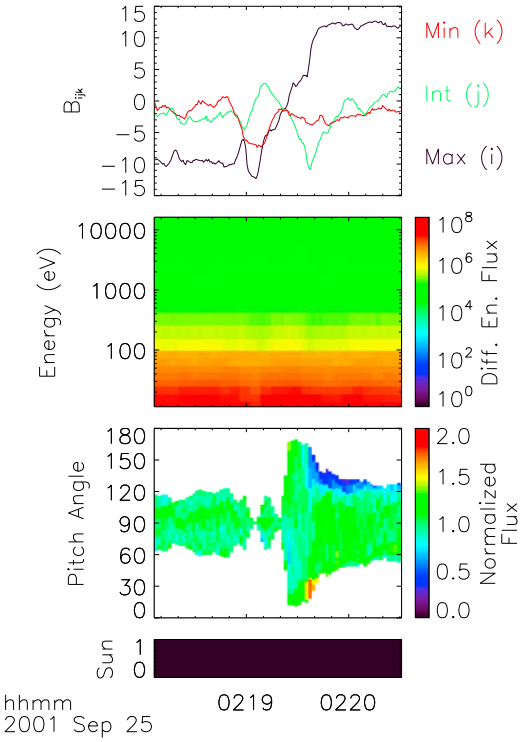

Figure 16. Nightside current sheet crossing at 02:19:23 UT on 2001/09/25, showing magnetic field in minimum variance coordinates, electron differential energy flux in ev(eV cm^2 s sr), normalized pitch angle distribution at 115 eV, and color bar showing spacecraft illumination (red is the sun, black is the shadow). Minimum variance analysis for this time period indicates principal component axes i,j,k = [0.78, −0.59, −0.13], [−0.22, −0.49, 0.84], [−0.56, −0.64, −.052] in MSO coordinates, with eigenvalues λ_i = 79, λ_j = 9.0, λ_k = 1.8. Magnetic field components suggest a crossing of type 4, antisunward from the X line.

agrees with that inferred from magnetic field components, but sometimes it does not, with no clear pattern. These discrepancies may result in part from incomplete pitch angle coverage, but likely also indicate electron physics not yet completely understood. We therefore use magnetic field components as our primary method of inferring the crossing location relative to the X line, but we also list the results from the electrons in Table 1.

[40] As Figure 14 shows, all the events we identified have main field directions consistent with the average draping pattern at Mars [*Halekas and Brain*, 2009], suggesting that we require no unusual solar wind magnetic field or magnetospheric configuration to produce a current sheet at which reconnection can occur. This holds equally true for crossings for which we infer a location sunward or antisunward from the X line. We do note that two of the three nightside crossings antisunward from the X line have main field axes which drape nearly horizontally compared to Mars's surface, rather than lying along the Mars-Sun line. We find this tendency encouraging, since this allows more room for an X line to fit between the spacecraft location and the collisional exosphere. In addition, current sheet magnetic field lines may curve away from the planet sunward from the crossings, avoiding any difficulty.

[41] Meanwhile, given the geographic locations of the current sheet crossings (shown in Figure 15 and listed in Table 1) and of the subsolar point during the crossing (listed in Table 1), we find no clear association with crustal fields. We do note some clustering for different types of events. All but one of the terminator/polar region events antisunward from an X line lie in the far southern hemisphere. In each of these cases, the crossing takes place antisunward from a region with significant crustal fields, suggesting a formation mechanism that involves crustal magnetic fields. On the other hand, most of the other events, regardless of SZA, tend to lie in the northern plains, and have no clear association with crustal fields. Thus, we may require multiple scenarios to explain the formation of the current sheets in which we observe signatures of reconnection.

4.4. Event Type Examples

[42] We display representative examples of each of the three remaining basic types of event that we observed (nightside antisunward and terminator/polar region sunward and antisunward), plus the lone dayside event, in Figures 16–19. First, Figure 16 shows a nightside event with an inferred location antisunward from the X line, with a roughly isotropic electron distribution near the crossing (at least

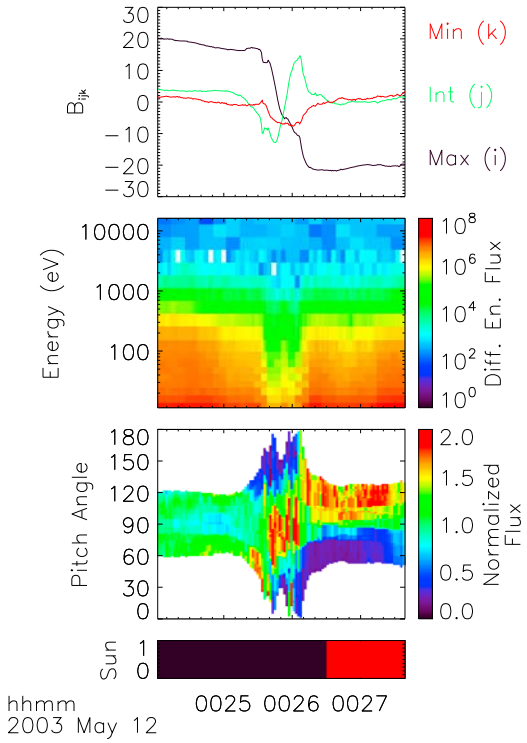

Figure 17. Terminator/polar region current sheet crossing at 00:25:53 UT on 2003/05/12, showing magnetic field in minimum variance coordinates, electron differential energy flux in ev(eV cm^2 s sr), normalized pitch angle distribution at 115 eV, and color bar showing spacecraft illumination (red is the sun, black is the shadow). Minimum variance analysis for this time period indicates principal component axes i,j,k = [0.96, 0.19, 0.22], [0.29, −0.58, −0.76], [−0.02, 0.79, −0.61] in MSO coordinates, with eigenvalues λ_i = 247, λ_j = 35.7, λ_k = 6.9. Magnetic field components suggest a crossing of type 1, sunward from the X line.

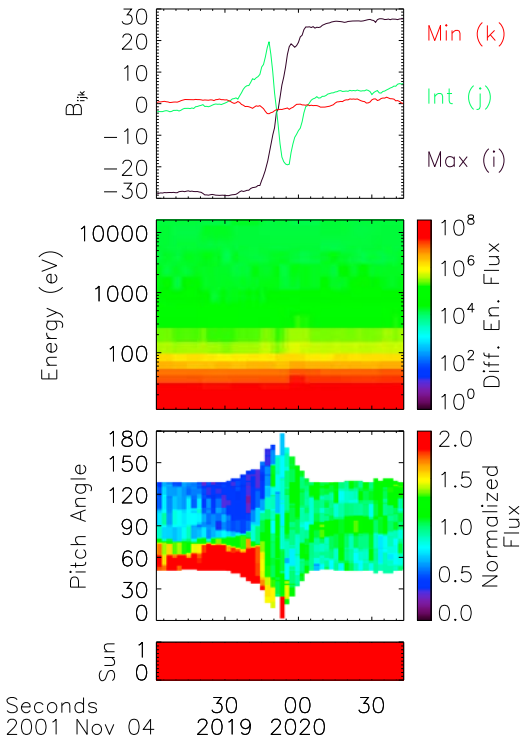

Figure 18. Terminator/polar region current sheet crossing at 20:19:51 UT on 2001/11/04, showing magnetic field in minimum variance coordinates, electron differential energy flux in ev(eV cm^2 s sr), normalized pitch angle distribution at 115 eV, and color bar showing spacecraft illumination (red is the sun, black is the shadow). Minimum variance analysis for this time period indicates principal component axes i,j,k = [0.90, −0.14, 0.42], [0.36, −0.29, −0.89], [0.25, 0.95, −0.21] in MSO coordinates, with eigenvalues λ_i = 652, λ_j = 41.4, λ_k = 1.41. Magnetic field components suggest a crossing of type 4, antisunward from the X line.

for the limited pitch angle range covered at this time). We find a loss cone distribution on one side, consistent with nearby field lines that pass through the collisional exosphere sunward from the crossing. We note the presence of a small flux rope signature just before the crossing, at ∼18:55, possibly analogous to the event described by *Eastwood et al.* [2008].

[43] Next, in Figure 17, we show a terminator/polar region crossing with an inferred location sunward from an X line. Similar to the nightside cases sunward from the X line described above, we observe a clear bifurcated minimum in the electron fluxes, with trapped electron distributions in the current sheet. These trapped electrons could represent a residual population of electrons remaining on field lines closed at the X line at the antisunward end and passing through the exosphere at the sunward end. We observe a similar phenomenon for other events sunward of X lines, and discuss the possible explanations further in Section 4.5 below.

[44] In Figure 18, we show a terminator/polar region crossing with an inferred location antisunward from an X line. Similar to the nightside case shown in Figure 16, this crossing has isotropic electrons in the current sheet and after the crossing, with a very slight increase in flux in the current sheet. Before the crossing, we observe field-aligned electrons flowing anti-sunward (away from the X line). These could represent part of the Hall current loop structure, but we cannot draw any strong conclusions as to their nature.

[45] Finally, in Figure 19 we show the lone crossing observed at a solar zenith angle less than seventy degrees. During this crossing, the electron distributions are very noisy, and we find it difficult to draw any firm conclusions as to the nature of this event. We note an interesting oscillation in the electron signature and magnetic field after the crossing, possibly indicating a boundary layer instability or turbulence.

4.5. Electron Characteristics

[46] Table 1 shows the properties of 115 eV electrons in and around the current sheet for each of the crossings. We note a very encouraging consistency in the electron characteristics observed for each type of event. As previously noted, the incomplete pitch angle coverage of the MGS ER renders these conclusions tentative, but since most of the results described below rely as much on total fluxes as pitch angle information, these conclusions may prove more robust than those derived purely from pitch angle information – as suggested by their surprising and impressive consistency.

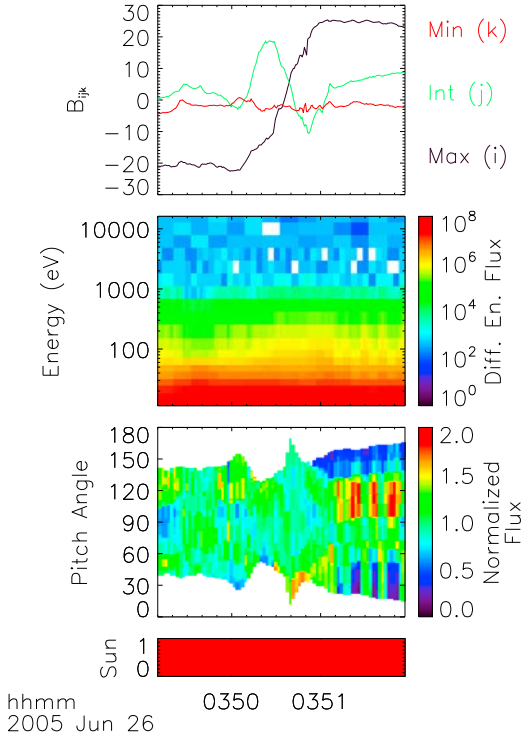

Figure 19. Dayside current sheet crossing at 03:50:38 UT on 2005/06/26, showing magnetic field in minimum variance coordinates, electron differential energy flux in ev(eV cm^2 s sr), normalized pitch angle distribution at 115 eV, and color bar showing spacecraft illumination (red is the sun, black is the shadow). Minimum variance analysis for this time period indicates principal component axes i,j,k = [.74, −.18, −.65], [.45, .85, .28], [.50, −.50, .71] in MSO coordinates, with eigenvalues λ_i = 426, λ_j = 36.2, λ_k = 1.05. Magnetic field components suggest a crossing of type 4, antisunward from the X line.

[47] We find that all crossings antisunward from the magnetic X line have roughly isotropic distributions in the current sheet, with some tendency for an increase in electron flux for nightside events, and most have isotropic and/or loss cone distributions before and after the crossing. On the other hand, crossings sunward from the X line tend to have isotropic or trapped distributions in the current sheet, with a strong tendency for a decrease in electron flux, and many have loss cone distributions and/or field-aligned electrons flowing sunward before and/or after the crossings.

[48] This consistent pattern of electron flux decreases for events sunward from the X line, and constant or increased electron fluxes antisunward from the X line, strongly suggests that we have correctly identified the locations of most current sheet crossings with respect to the magnetic X line, lending further support to our contentions that the current sheet does not often overtake the spacecraft, and that magnetic field components provide a more reliable method for locating the X line than electron pitch angle distributions.

[49] We can draw several physical conclusions from the electron signatures. First, the almost universal decrease in electron flux observed sunward from X lines, both on the night side and in the terminator/polar regions, suggests that these crossings take place on flux tubes from which plasma has at least partially been removed. We can explain these observations in terms of a scenario of flux tubes closed at an X line at the antisunward end, and connected to the collisional exosphere at the sunward end (possibly, but not necessarily, via crustal magnetic field lines). The prevalence of loss cone distributions (suggesting magnetic connection to the collisional exosphere) and field-aligned electrons flowing sunward on either side of the current sheet strengthen this conclusion. Thus, we suggest that these events represent cases where a current sheet forms either via interaction with crustal fields or directly by draping of antiparallel magnetic fields, on field lines that pass through the collisional exosphere at the sunward end. Then a reconnection X line forms antisunward from the crossing location, leading to a closed field geometry, plasma loss, and partial or full evacuation of the field lines near the neutral sheet location.

[50] Meanwhile, for events located antisunward from magnetic X lines, we observe either relatively constant electron flux, or an increase in electron flux. We can explain the lack of a decrease in electron flux (though perhaps not the increase in flux sometimes observed) in terms of a scenario with magnetic field lines closed at an X line on the sunward end, but open on the antisunward end. Thus, electrons would have free access to the crossing from the Martian magnetotail or from the solar wind, depending on the global magnetospheric topology. The tendency for loss cone distributions before and/or after these crossings is not inconsistent with this picture, since these nearby magnetic field lines could pass through the collisional exosphere sunward from the X line location, without affecting electron access to these regions from the antisunward end.

4.6. Current Sheet Properties

[51] Given the large data set of current sheet crossings from a previous survey [*Halekas and Brain*, 2009], we can easily compare the basic properties of the current sheets identified in this study with those of the very much larger population of current sheets observed during the MGS mapping mission, utilizing the same methodology as used by *Halekas and Brain* [2009] to determine current sheet properties. For the most part, we do not find any significant differences between the 26 events considered in this study and the larger population of current sheets observed by MGS. The median magnitude of the main, normal, and guide fields for the selected events corresponds relatively closely to the overall values. However, we do find that the current sheets identified in this study have a median minimum thickness of only 67 km, compared to the median minimum thickness for all current sheets of 174 km. While we note a relatively wide range of current sheet thicknesses even in our small sample, and must always admit some level of ambiguity due to the possibility of current sheet motion, the fact that the inferred minimum thicknesses of these current sheets tend to be smaller than average suggests that thin current sheets at Mars favor the occurrence of reconnection, just as we expect from theory and modeling.

4.7. External Drivers

[52] We can similarly investigate external drivers, especially solar wind conditions, for all events. Again, we find few obvious differences, and none that correspond to season or IMF draping direction. However, we do find a median subsolar magnetic field strength (a useful proxy for solar wind dynamic pressure [*Brain et al.*, 2005]) of 50 nT, somewhat larger than the overall median value of 36 nT. This may suggest that higher solar wind dynamic pressures, which would tend to compress draped field lines around Mars, produce a current sheet configuration more favorable for reconnection.

[53] Finally, we find a tendency for only small changes in IMF draping direction occurring around the times of our events, with the median change in IMF draping azimuth from orbit to orbit for our events only 18°, as compared to 40° for the whole population of current sheets. This argues strongly against an origin related to solar wind discontinuities for most of the current sheets in question, and instead suggests that a steady draping pattern may produce a current sheet configuration more favorable for reconnection.

5. Implications and Conclusions

[54] For a small fraction (~0.25%) of the current sheets encountered by MGS during its 400 km mapping orbit, we observe bipolar out-of-plane signatures similar to those predicted by modern computer simulations of collisionless reconnection, and observed at active reconnection sites in and near the terrestrial magnetosphere, as well as in the laboratory. The ratios of both normal and out-of-plane fields to the main field are very similar to those observed at Earth, though with somewhat larger than typical normal fields, possibly because of our selection criteria. These fields have polarities consistent with the effects of differential ion and electron motion near a magnetic X line and the resulting Hall currents in the reconnection diffusion region, suggesting that the spacecraft passes through or very near the ion diffusion region at these times, and that collisionless reconnection in current sheets occurs at Mars as well as at the Earth.

[55] We find 26 clear examples of this unique signature in the MGS data, out of a data set of over 10,000 current sheet encounters. Our selection criteria ensure that we have only considered relatively intense reconnection events, so many more events may occur than considered here; however, the number of events for which we can clearly identify reconnection signatures proves quite small. This may therefore either suggest that reconnection is rare at Mars, that the reconnection diffusion region is small and rarely encountered, that reconnection at Mars rarely produces large out-of-plane magnetic signatures, or that reconnection is rare at MGS mapping altitude. Given the ever changing magnetic topology and the complex interplay between solar wind, crustal, and draped magnetospheric field lines at Mars, we suspect that reconnection should actually prove relatively common in the Martian magnetosphere. At Earth, we have few in situ observations of Hall magnetic fields in reconnection diffusion regions, but it is still commonly accepted that reconnection occurs frequently. Similarly, the small number of events found at Mars should not lead us to conclude that reconnection is unimportant in the Martian magnetosphere. Indeed, given the small size of the reconnection diffusion region, we would find it surprising if we observed its signatures more frequently than we do at Mars – the number of events we observe may even imply that reconnection is very common in the Martian magnetosphere. We will likely need both global and local simulations of a dynamic (rather than steady state) Martian magnetosphere in order to place these observations into a global context.

[56] Compared to many reconnection diffusion region crossings in the terrestrial magnetotail, we observe remarkably smooth magnetic signatures at Mars, suggesting less turbulence and/or current sheet motion than at the Earth. In part, this may result from the basic properties of the Martian magnetotail – or a general property of induced magnetospheres. Previous studies [*Halekas et al.*, 2006, 2008] have found little consistent signature of increased electron fluxes or electron acceleration at most Martian magnetotail current sheet crossings, suggesting a quieter plasma sheet environment than at Earth. Thus, Mars may prove a very good environment in which to study the microphysics of reconnection with future missions.

[57] Though some of our events occur downstream from significant crustal field regions, we do not observe a clear and consistent association with crustal fields, suggesting that they do not always play a significant role in current sheet formation. Likewise, the small inferred changes in IMF clock angle during event periods suggests that solar wind discontinuities also do not play a significant role in current sheet formation for these events. Therefore, we conclude that magnetic field draping in the induced magnetosphere of Mars alone may prove sufficient to produce current sheets capable of reconnection. The increased solar wind dynamic pressure during events suggests that a more compressed draping configuration may increase the chances of reconnection, consistent with this picture.

[58] If reconnection could be shown to be a common process in the Martian magnetosphere, it would have significant implications for atmospheric loss, since it provides a possible mechanism to liberate large populations of ions of planetary origin from the Martian magnetosphere. This study does not indicate that such a process is common at Mars, but it also does not rule out such a scenario. Before we can conclusively determine the importance of reconnection in the Martian magnetosphere, we will need much more comprehensive measurements of magnetic fields, ions, and electrons at a variety of altitudes (as well as sophisticated simulations to place these observations in context). The upcoming MAVEN mission will provide just such data.

[59] **Acknowledgments.** This work was supported by NASA grant NNX08AK95G. We dedicate this paper to the memory of Mario Acuña, without whose vision and tireless effort the MGS MAG/ER experiment would never have flown.

[60] Wolfgang Baumjohann thanks Martin Volwerk and another reviewer for their assistance in evaluating this manuscript.

References

Acuña, M. H., et al. (1999), Global distribution of crustal magnetization found by the Mars Global Surveyor MAG/ER experiment, *Science*, *284*, 790–793, doi:10.1126/science.284.5415.790.

Acuña, M. H., et al. (2001), The magnetic field of Mars: Summary of results from the aerobraking and mapping orbits, *J. Geophys. Res.*, *106*, 23,403–23,418, doi:10.1029/2000JE001404.

Alexeev, I. V., C. J. Owen, A. N. Fazakerley, A. Runov, J. P. Dewhurst, A. Balogh, H. Reme, B. Klecker, and L. Kistler (2005), Cluster observations of currents in the plasma sheet during reconnection, *Geophys. Res. Lett.*, *32*, L03101, doi:10.1029/2004GL021420.

Bertucci, C., C. Mazelle, M. H. Acuña, C. T. Russell, and J. A. Slavin (2003), Magnetic field draping enhancement at the Martian magnetic pileup boundary from Mars Global Surveyor observations, *Geophys. Res. Lett.*, *30*(2), 1099, doi:10.1029/2002GL015713.

Birn, J., et al. (2001), Geospace Environmental Modeling (GEM) magnetic reconnection challenge, *J. Geophys. Res.*, *106*, 3715–3719, doi:10.1029/1999JA900449.

Borg, A. L., M. Øieroset, T. Phan, F. S. Mozer, A. Pedersen, C. Mouikis, J. P. McFadden, C. Twitty, A. Balogh, and H. Rème (2005), Cluster encounter of a magnetic reconnection diffusion region in the near-Earth magnetotail on September 19, 2003, *Geophys. Res. Lett.*, *32*, L19105, doi:10.1029/2005GL023794.

Brain, D. A., J. S. Halekas, R. J. Lillis, D. L. Mitchell, R. P. Lin, and D. H. Crider (2005), Variability of the altitude of the Martian sheath, *Geophys. Res. Lett.*, *32*, L18203, doi:10.1029/2005GL023126.

Brain, D. A., J. S. Halekas, L. M. Peticolas, R. P. Lin, J. G. Luhmann, D. L. Mitchell, G. T. Delory, S. W. Bougher, M. H. Acuña, and H. Réme (2006), On the origin of aurorae at Mars, *Geophys. Res. Lett.*, *33*, L01201, doi:10.1029/2005GL024782.

Brain, D. A., R. J. Lillis, D. L. Mitchell, J. S. Halekas, and R. P. Lin (2007), Electron pitch angle distributions as indicators of magnetic topology near Mars, *J. Geophys. Res.*, *112*, A09201, doi:10.1029/2007JA012435.

Cain, J. C., B. B. Ferguson, and D. Mozzoni (2003), An $n = 90$ internal potential function of the Martian crustal magnetic field, *J. Geophys. Res.*, *108*(E2), 5008, doi:10.1029/2000JE001487.

Cloutier, P. A., et al. (1999), Venus-like interaction of the solar wind with Mars, *Geophys. Res. Lett.*, *26*, 2685–2688, doi:10.1029/1999GL900591.

Crider, D. H., et al. (2002), Observations of the latitude dependence of the location of the Martian magnetic pileup boundary, *Geophys. Res. Lett.*, *29*(11), 1170, doi:10.1029/2001GL013860.

Crider, D. H., D. A. Brain, M. H. Acuña, D. Vignes, C. Mazelle, and C. Bertucci (2004), Mars Global Surveyor observations of solar wind magnetic field draping around Mars, *Space Sci. Rev.*, *111*, 203–221, doi:10.1023/B:SPAC.0000032714.66124.4e.

Deng, H., H. Matsumoto, H. Kojima, T. Mukai, R. R. Anderson, W. Baumjohann, and R. Nakamura (2004), Geotail encounter with reconnection diffusion region in the Earth's magnetotail: Evidence of multiple X lines collisionless reconnection?, *J. Geophys. Res.*, *109*, A05206, doi:10.1029/2003JA010031.

Dubinin, E., R. Lundin, O. Norberg, and N. Pissarenko (1993), Ion acceleration in the Martian tail: Phobos observations, *J. Geophys. Res.*, *98*, 3991–3997, doi:10.1029/92JA02233.

Dubinin, E., R. Lundin, and K. Schwingenschuh (1994), Solar wind electrons as tracers of the Martian magnetotail topology, *J. Geophys. Res.*, *99*, 21,233–21,240, doi:10.1029/94JA01271.

Dungey, J. W. (1961), Interplanetary magnetic field and the auroral zones, *Phys. Rev. Lett.*, *6*, 47–48, doi:10.1103/PhysRevLett.6.47.

Eastwood, J. P., T. D. Phan, F. S. Mozer, M. A. Shay, M. Fujimoto, A. Retino, M. Hesse, A. Balogh, E. A. Lucek, and I. Dandouras (2007), Multi-point observations of the Hall electromagnetic field and secondary

island formation during magnetic reconnection, *J. Geophys. Res.*, *112*, A06235, doi:10.1029/2006JA012158.

Eastwood, J. P., D. A. Brain, J. S. Halekas, J. F. Drake, T. D. Phan, M. Øieroset, D. L. Mitchell, R. P. Lin, and M. Acuña (2008), Evidence for collisionless magnetic reconnection at Mars, *Geophys. Res. Lett.*, *35*, L02106, doi:10.1029/2007GL032289.

Elphic, R. C., C. A. Cattell, K. Takahashi, S. J. Bame, and C. T. Russell (1986), ISEE-1 and 2 observations of magnetic flux ropes in the magnetotail: FTE's in the plasma sheet?, *Geophys. Res. Lett.*, *13*, 648–651, doi:10.1029/GL013i007p00648.

Fedorov, A., et al. (2006), Structure of the Martian wake, *Icarus*, *182*, 329–336, doi:10.1016/j.icarus.2005.09.021.

Fedorov, A., et al. (2008), Comparative analysis of Venus and Mars magnetotails, *Planet. Space Sci.*, *56*, 812–817, doi:10.1016/j.pss.2007.12.012.

Ferguson, B., J. C. Cain, D. H. Crider, E. Harnett, and D. A. Brain (2005), External fields on the night-side of Mars at Mars Global Surveyor mapping altitudes, *Geophys. Res. Lett.*, *32*, L16105, doi:10.1029/2004GL021964.

Franz, M., E. Dubinin, E. Roussos, J. Woch, J. D. Winningham, R. Frahm, A. J. Coates, A. Fedorov, S. Barabash, and R. Lundin (2006), Plasma moments in the environment of Mars: Mars Express ASPERA-3 observations, *Space Sci. Rev.*, *126*, 165–207, doi:10.1007/s11214-006-9115-9.

Fujimoto, M., M. S. Nakamura, I. Shinohara, T. Nagai, T. Mukai, Y. Saito, T. Yamamoto, and S. Kokubun (1997), Observations of earthward streaming electrons at the trailing boundary of a plasmoid, *Geophys. Res. Lett.*, *24*, 2893–2896, doi:10.1029/97GL02821.

Gosling, J. T. (1990), Coronal mass ejections and magnetic flux ropes in interplanetary space, in *Physics of Magnetic Flux Ropes*, *Geophys. Monogr. Ser.*, vol. 58, edited by C. T. Russell et al., pp. 343–364, AGU, Washington, D. C.

Gosling, J. T., S. J. Bame, W. C. Feldman, D. J. McComas, J. L. Phillips, and B. E. Goldstein (1993), Counterstreaming suprathermal electron events upstream of corotating shocks in the solar wind beyond −2 AU, Ulysses, *Geophys. Res. Lett.*, *20*, 2335–2338, doi:10.1029/93GL02489.

Gosling, J. T., R. M. Skoug, D. J. McComas, and C. W. Smith (2005), Magnetic disconnection from the Sun: Observations of a reconnection exhaust in the solar wind at the heliospheric current sheet, *Geophys. Res. Lett.*, *32*, L05105, doi:10.1029/2005GL022406.

Halekas, J. S., and D. A. Brain (2009), Global distribution, structure, and solar wind control of low altitude current sheets at Mars, *Icarus*, doi:10.1016/j.icarus.2008.12.032, in press.

Halekas, J. S., D. A. Brain, R. J. Lillis, M. O. Fillingim, D. L. Mitchell, and R. P. Lin (2006), Current sheets at low altitudes in the Martian magnetotail, *Geophys. Res. Lett.*, *33*, L13101, doi:10.1029/2006GL026229.

Halekas, J. S., D. A. Brain, R. P. Lin, J. G. Luhmann, and D. L. Mitchell (2008), Distribution and variability of accelerated electrons at Mars, *Adv. Space Res.*, *41*, 1347–1352, doi:10.1016/j.asr.2007.01.034.

Hesse, M., J. Birn, and M. Kuznetsova (2001), Collisionless magnetic reconnection: Electron processes and transport modeling, *J. Geophys. Res.*, *106*, 3721–3735, doi:10.1029/1999JA001002.

Hones, E. W., Jr., J. Birn, S. J. Bame, and C. T. Russell (1983), New observations of plasma vortices and insights into their interpretation, *Geophys. Res. Lett.*, *10*, 674–677, doi:10.1029/GL010i008p00674.

Hoshino, M., T. Mukai, T. Terasawa, and I. Shinohara (2001), Suprathermal electron acceleration in magnetic reconnection, *J. Geophys. Res.*, *106*(A11), 25,979–25,997, doi:10.1029/2001JA900052.

Ip, W.-H. (1992), Ion acceleration at the current sheet of the Martian magnetosphere, *Geophys. Res. Lett.*, *19*, 2095–2098, doi:10.1029/92GL02098.

Krymskii, A. M., T. K. Breus, N. F. Ness, M. H. Acuña, J. E. P. Connerney, D. H. Crider, D. L. Mitchell, and S. J. Bauer (2002), Structure of the magnetic field fluxes connected with crustal magnetization and topside ionosphere at Mars, *J. Geophys. Res.*, *107*(A9), 1245, doi:10.1029/2001JA000239.

Lichtenegger, H., K. Schwingenschuh, E. Dubinin, and R. Lundin (1995), Particle simulation in the Martian magnetotail, *J. Geophys. Res.*, *100*, 21,659–21,667, doi:10.1029/95JA01830.

Luhmann, J. G. (1990), A model of the ion wake of Mars, *Geophys. Res. Lett.*, *17*, 869–872, doi:10.1029/GL017i006p00869.

Lundin, R., H. Borg, B. Hultqvist, A. Zakharov, and R. Pellinen (1989), First measurements of the ionospheric plasma escape from Mars, *Nature*, *341*, 609–612, doi:10.1038/341609a0.

Lundin, R., et al. (2006), Plasma acceleration above Martian magnetic anomalies, *Science*, *311*, 980–983, doi:10.1126/science.1122071.

Manapat, M., M. Øieroset, T. D. Phan, R. P. Lin, and M. Fujimoto (2006), Field-aligned electrons at the lobe/plasma sheet boundary in the mid-to-distant magnetotail and their association with reconnection, *Geophys. Res. Lett.*, *33*, L05101, doi:10.1029/2005GL024971.

Mitchell, D. L., et al. (2001), Probing Mars' crustal magnetic field and ionosphere with the MGS Electron Reflectometer, *J. Geophys. Res.*, *106*, 23,419–23,427, doi:10.1029/2000JE001435.

Mozer, F. S., S. D. Bale, and T. D. Phan (2002), Evidence of diffusion regions at a subsolar magnetopause crossing, *Phys. Rev. Lett.*, *89*, 015002.1–015002.4, doi:10.1103/PhysRevLett.89.015002.

Nagai, T., I. Shinohara, M. Fujimoto, M. Hoshino, Y. Saito, S. Machida, and T. Mukai (2001), Geotail observations of the Hall current system: Evidence of magnetic reconnection in the magnetotail, *J. Geophys. Res.*, *106*, 25,929–25,949, doi:10.1029/2001JA900038.

Nagai, T., I. Shinohara, M. Fujimoto, S. Machida, R. Nakamura, Y. Saito, and T. Mukai (2003), Structure of the Hall current system in the vicinity of the magnetic reconnection site, *J. Geophys. Res.*, *108*(A10), 1357, doi:10.1029/2003JA009900.

Nagy, A. F., et al. (2004), The plasma environment of Mars, *Space Sci. Rev.*, *111*, 33–114, doi:10.1023/B:SPAC.0000032718.47512.92.

Øieroset, M., T. D. Phan, M. Fujimoto, R. P. Lin, and R. P. Lepping (2001), In situ detection of collisionless reconnection in the Earth's magnetotail, *Nature*, *412*, 414–417, doi:10.1038/35086520.

Owen, C. J., J. A. Slavin, N. Fazkerley, M. W. Dunlop, and A. Balogh (2005), Cluster electron observations of the separatrix layer during traveling compression regions, *Geophys. Res. Lett.*, *32*, L03104, doi:10.1029/2004GL021767.

Paschmann, G., B. U. Ö. Sonnerup, I. Papamastorakis, N. Schopke, and G. Haerendel (1979), Plasma acceleration at the Earth's magnetopause: evidence for reconnection, *Nature*, *282*, 243–246, doi:10.1038/282243a0.

Phan, T. D., G. Paschmann, C. Twitty, F. S. Mozer, J. T. Gosling, J. P. Eastwood, M. Øieroset, H. Reme, and E. A. Leuck (2007), Evidence for magnetic reconnection initiated in the magnetosheath, *Geophys. Res. Lett.*, *34*, L14104, doi:10.1029/2007GL030343.

Pritchett, P. L. (2001a), Collisionless magnetic reconnection in a three-dimensional open system, *J. Geophys. Res.*, *106*, 25,961–25,977, doi:10.1029/2001JA000016.

Pritchett, P. L. (2001b), Geospace Environment Modeling magnetic reconnection challenge: Simulations with a full particle electromagnetic code, *J. Geophys. Res.*, *106*, 3783–3798, doi:10.1029/1999JA001006.

Ren, Y., M. Yamada, S. Gerhardt, J. Hantao, R. Kulsrud, and A. Kuritsyn (2005), Experimental verification of the Hall effect during magnetic reconnection in a laboratory plasma, *Phys. Rev. Lett.*, *95*, 055003.1–055003.4, doi:10.1103/PhysRevLett.95.055003.

Riedler, W., K. Schwingenschuh, H. Lichtenegger, D. Mohlmann, J. Rustenbach, Y. Yeroshenko, J. Achache, J. Slavin, J. G. Luhmann, and C. T. Russell (1991), Interaction of the solar wind with the planet Mars: Phobos 2 magnetic field observations, *Planet. Space Sci.*, *39*, 75–81, doi:10.1016/0032-0633(91)90129-X.

Rosenbauer, H., N. Shutte, A. Galeev, K. Gringauz, and I. Apathy (1989), Ions of Martian origin and plasma sheet in the Martian magnetosphere: Initial results of the TAUS experiment, *Nature*, *341*, 612–614, doi:10.1038/341612a0.

Runov, A., et al. (2003), Current sheet structure near magnetic X-line observed by Cluster, *Geophys. Res. Lett.*, *30*(11), 1579, doi:10.1029/2002GL016730.

Russell, C. T., and R. C. Elphic (1978), Initial ISEE magnetometer results–Magnetopause observations, *Space Sci. Rev.*, *22*, 681–715, doi:10.1007/BF00212619.

Shay, M. A., J. F. Drake, R. E. Denton, and D. Biskamp (1998), Structure of the dissipation region during collisionless magnetic reconnection, *J. Geophys. Res.*, *103*, 9165–9176, doi:10.1029/97JA03528.

Shay, M. A., J. F. Drake, B. N. Rogers, and R. E. Denton (2001), Alfvénic collisionless magnetic reconnection and the Hall term, *J. Geophys. Res.*, *106*, 3759–3772, doi:10.1029/1999JA001007.

Slavin, J. A., E. J. Smith, B. T. Tsuratani, D. G. Sibeck, H. J. Singer, D. N. Baker, J. T. Gosling, E. W. Hones, and F. L. Scarf (1984), Substorm associated traveling compression regions in the distant tail–ISEE-3 geotail observations, *Geophys. Res. Lett.*, *11*, 657–660, doi:10.1029/GL011i007p00657.

Slavin, J. A., E. J. Smith, D. G. Sibeck, D. N. Baker, R. D. Zwickl, and S.-I. Akasofu (1985), An ISEE-3 study of average and substorm conditions in the distant magnetotail, *J. Geophys. Res.*, *90*, 10,875–10,895, doi:10.1029/JA090iA11p10875.

Sonnerup, B. U. Ö. (1979), Magnetic field reconnection, in *Solar System Plasma Physics*, vol. *3*, edited by E. N. Parker, C. F. Kennel, and L. T. Lanzerotti, pp. 47–108, North-Holland, Amsterdam.

Sonnerup, B. U. Ö., and L. J. Cahill Jr. (1967), Magnetopause structure and attitude from Explorer 12 observations, *J. Geophys. Res.*, *72*, 171–183, doi:10.1029/JZ072i001p00171.

Sonnerup, B. U. Ö., G. Paschmann, I. Papamastorakis, N. Sekopke, G. Haerendel, S. J. Bame, J. R. Ashbridge, J. T. Gosling, and C. T. Russell (1981), Evidence for magnetic field reconnection at the Earth's

magnetopause, *J. Geophys. Res.*, *86*, 10,049–10,067, doi:10.1029/JA086iA12p10049.

Spreiter, J. R., and S. S. Stahara (1992), Computer modeling of the solar wind interaction with Venus and Mars, in *Venus and Mars: Atmospheres, Ionospheres, and Solar Wind Interactions*, *Geophys. Monogr. Ser.*, vol. 66, edited by J. G. Luhmann et al., pp. 345–383, AGU, Washington, D. C.

Terasawa, T. (1983), Hall current effect on tearing mode instability, *Geophys. Res. Lett.*, *10*, 475–478, doi:10.1029/GL010i006p00475.

Treumann, R. A., C. H. Jaroschek, R. Nakamura, A. Runov, and M. Scholer (2006), The role of the Hall effect in collisionless magnetic reconnection, *Adv. Space Res.*, *38*, 101–111, doi:10.1016/j.asr.2004.11.045.

Uluşen, D., and I. Linscott (2008), Low-energy electron current in the Martian tail due to reconnection of draped interplanetary magnetic field and crustal magnetic fields, *J. Geophys. Res.*, *113*, E06001, doi:10.1029/2007JE002916.

Vaivads, A., Y. Khotyaintsev, M. André, A. Retinò, S. Buchert, B. N. Rogers, P. Décréau, G. Paschmann, and T. D. Phan (2004), Structure of the magnetic reconnection diffusion region from four-spacecraft observations, *Phys. Rev. Lett.*, *93*, 105001.1–105001.4, doi:10.1103/PhysRevLett.93.105001.

Vasyliunas, V. M. (1975), Theoretical models of magnetic field line merging, *Rev. Geophys. Space Phys.*, *13*, 303–336, doi:10.1029/RG013i001p00303.

Yang, H. A., S. P. Jin, and G. C. Zhou (2006), Density depletion and Hall effect in magnetic reconnection, *J. Geophys. Res.*, *111*, A11223, doi:10.1029/2005JA011536.

Yeroshenko, Y., W. Riedler, K. I. Schwingenschuh, J. G. Luhmann, M. Ong, and C. T. Russell (1990), The magnetotail of Mars: Phobos observations, *Geophys. Res. Lett.*, *17*, 885–888, doi:10.1029/GL017i006p00885.

D. A. Brain, J. P. Eastwood, J. S. Halekas, R. P. Lin, M. Øieroset, and T. D. Phan, Space Sciences Laboratory, University of California, 7 Gauss Way, Berkeley, CA 94720, USA. (jazzman@ssl.berkeley.edu)